RSC Advances

REVIEW

View Article Online
View Journal | View Issue

Cite this: *RSC Adv.*, 2025, **15**, 22097

Synthesis and SARs of benzimidazoles: insights into antimicrobial innovation (2018–2024)

Ahmed A. Ibrahim,*[a] Eman G. Said,[b] Asmaa M. AboulMagd,[a] Noha H. Amin[b] and Hamdy M. Abdel-Rahman*[cd]

Benzimidazole derivatives have garnered significant attention in medicinal chemistry owing to their versatile pharmacological properties, particularly their potent antimicrobial activity. This review comprehensively explores the advancements in the synthesis of benzimidazoles and their antimicrobial property evaluation from 2018 to 2024. Recent synthetic methodologies emphasize green chemistry approaches including solvent-free and catalyst-driven reactions, offering improved yields, selectivity, and environmental sustainability. Structural modifications, such as functionalization at positions 2 and 5/6 of the benzimidazole ring, were extensively investigated to enhance the antimicrobial efficacy against a broad spectrum of pathogens including multidrug-resistant bacterial and fungal strains. Furthermore, we elucidate the structure–activity relationships (SARs) of benzimidazole derivatives, enabling the rational design of highly potent antimicrobial agents. The mentioned period also witnessed the integration of hybrid molecules, wherein benzimidazoles were conjugated with other bioactive scaffolds to achieve synergistic antimicrobial effects.

Received 3rd February 2025
Accepted 6th June 2025

DOI: 10.1039/d5ra00819k

rsc.li/rsc-advances

1 Introduction

The history of heterocyclic chemistry first began in the 1800s alongside the progress of organic chemistry.[1] Since 2020, nearly 65% of the literature in organic chemistry is based on heterocyclic chemistry.[2] Heterocycles have important applications in the fields of chemistry, industry, and biology, as they play vital roles in the metabolic processes of all living cells.[3] They typically consist of five- or six-membered rings and have at least one heteroatom, such as a nitrogen (N), oxygen (O), or sulfur (S) atom.[4] Nitrogenous heterocyclic compounds have a significant influence in the process of discovering and developing drugs, primarily because they are commonly found in natural products and bioactive molecules.[5] These compounds frequently exhibit a wide range of unique pharmacological effects, which make them interesting for researchers.[6] Particularly, the benzimidazole ring has been extensively investigated in the field of medicinal chemistry since 1944,[7] following the discovery of 5,6-dimethylbenzimidazole as a byproduct of vitamin B12 breakdown,[8] owing to its structure similarity with DNA-purine nitrogen bases (adenine and guanine), and it consists of a bicyclic organic structure having an imidazole ring that contains two nitrogen atoms attached to one benzene ring.[9,10] Multiple studies reported in the literature have presented an in-depth pharmacological framework of benzimidazoles and their derivatives,[11] exhibiting potential biological activities such as antibacterial,[12–14] antifungal,[15,16] antiviral,[17,18] antileishmanial,[19,20] antimalarial[21,22] and antiprotozoal[23,24] functions. Currently, several benzimidazole-based drugs are available and commercially accessible, including mebendazole **1** (ref. 25), ciclobendazole **2** (ref. 26), carbendazim **3** (ref. 27), albendazole **4** (ref. 28), thiabendazole **5** (ref. 29), chlormidazole **6** (ref. 30), fuberidazole **7** (ref. 31) and benomyl **8** (ref. 27)(Fig. 1).[32] Nevertheless, this review focused on the pharmacological properties of benzimidazole derivatives that have been evaluated between 2018 and 2024.

1.1 Chemistry

The systematic nomenclature of the 1*H*-benzimidazole ring system is illustrated in structure **9**. Although benzimidazole in **9** has been shown to have a proton at N1, there is, in fact, a quick exchange between the –NH– and =N-nitrogen atoms, allowing for the appearance of two tautomers of the benzimidazole molecule. Tautomerism develops *via* an intermolecular mechanism involving two benzimidazole molecules **9** and **9a** or upon interactions with a protic solvent like water[33] (Fig. 2).

1.2 Synthetic pathways

Due to the significant synthetic relevance and diverse bioactivities of benzimidazoles and their derivatives, efforts have been

[a]*Pharmaceutical Chemistry Department, Faculty of Pharmacy, Nahda University in Beni-Suef (NUB), Beni-Suef 62513, Egypt. E-mail: ahmed.abdelrazik@nub.edu.eg*
[b]*Medicinal Chemistry Department, Faculty of Pharmacy, Beni-Suef University, Beni-Suef 62514, Egypt*
[c]*Medicinal Chemistry Department, Faculty of Pharmacy, Assiut University, Assiut 71526, Egypt. E-mail: hamdym@aun.edu.eg*
[d]*Pharmaceutical Chemistry Department, Faculty of Pharmacy, Badr University in Assiut (BUA), Assiut 2014101, Egypt*

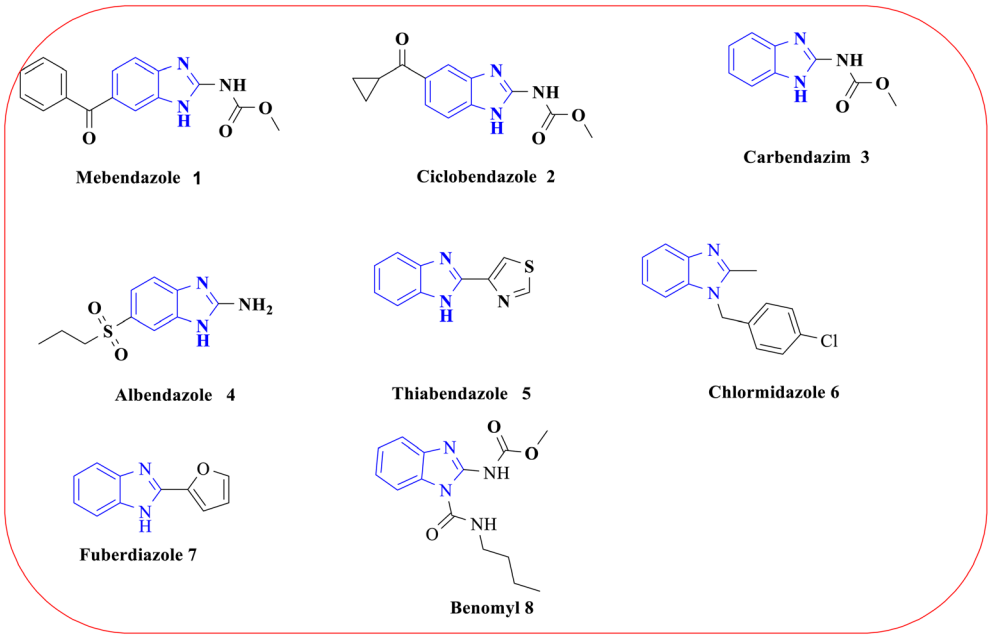

Fig. 1 Some commercially available benzimidazole-based drugs.

Fig. 2 Tautomerism of the benzimidazole nucleus.

consistently made to create libraries of these molecules. Numerous synthetic processes have been designed and modified to achieve products with high yield and purity. An initial review revealed that the first benzimidazole **12** or **13** was produced in 1872 by Hoebrecker *via* the reduction of 4-methyl-2-nitroacetanilide **10**.[34] After several years, Ladenburg synthesized compounds **12** or **13** with a moderate yield by refluxing 3,4-diaminotoluene **11** with acetic acid; the term 'Anhydrobase' originated in the early literature to describe the loss of water during the synthesis of this type of chemical reaction (Fig. 3).[35–37]

1.2.1 From carboxylic acids, esters or aldehydes. The primary synthesis methods for benzimidazole candidates *via* Phillip's method involve the condensation of *O*-phenylenediamine **14** with carboxylic acids **15**, esters **17** or aldehydes **19** by cyclization under high acidic conditions such as hydrochloric acid, hot glacial acetic acid or boric acid. This method is widely utilized for the synthesis of various benzimidazoles (Scheme 1).[38–40]

The proper imidate ester (trichloroacetimidate) **17** was employed as the starting material for the synthesis of benzimidazole derivatives by Alaqeel *via* reaction with *O*-phenylenediamine **14** or its salt to yield 2-trichloromethyl benzimidazole **18** at room temperature, which serves as a significant precursor for 2-carboxylic benzimidazoles with a good yield (Scheme 2).[41]

Benzimidazole derivative **20** can be synthesized from aldehydes, as reported by Heravi *et al.*, *via* straightforward one-step synthesis from *O*-phenylenediamine **14** and 2-

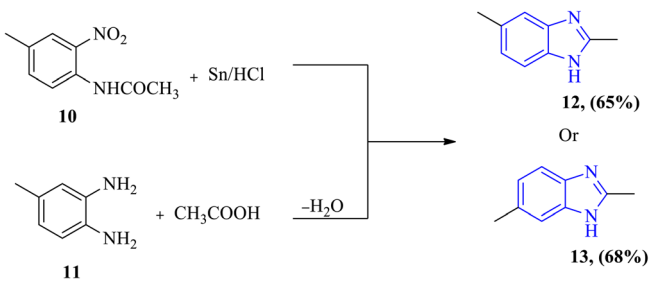

Fig. 3 The first schemes used for benzimidazole synthesis.

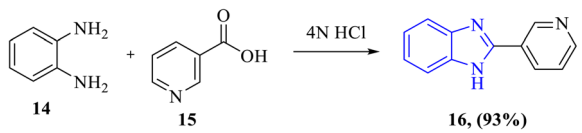

Scheme 1 Phillips method: synthesis of benzimidazole derivatives *via* the condensation of *O*-phenylenediamine **14** with carboxylic acids **15** under acidic conditions.

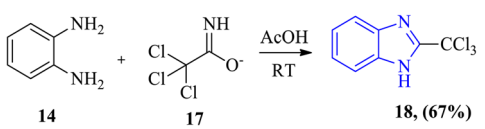

Scheme 2 Synthesis of 2-trichloromethyl benzimidazole **18** from *O*-phenylenediamine **14** and trichloroacetimidate ester **17** at room temperature.

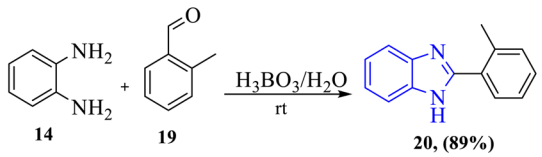

Scheme 3 One-step synthesis of benzimidazole derivative **20** from *O*-phenylenediamine **14** and 2-methylbenzaldehyde **19** using boric acid under mild aqueous conditions.

methylbenzaldehyde **19** in the presence of boric acid as an efficient catalyst under mild aqueous conditions (Scheme 3).[42]

1.2.2 Metal-catalyzed reactions. Metal-catalyzed reactions have emerged as a cornerstone in the synthesis of benzimidazole derivatives, providing efficient, selective, and versatile routes for constructing these biologically significant heterocycles. Transition metal catalysts such as palladium (Pd) and copper (Cu) play a pivotal role in facilitating key transformations including cyclization and functionalization of benzimidazole scaffolds.[43–45]

A metal-catalyzed reaction was demonstrated by Srimani *et al.* for the synthesis of benzimidazole through coupling aromatic diamines **14** with primary alcohols **21**, as illustrated in Scheme 4. This reaction employs a phosphine-free tridentate NNS–manganese(I) complex as a catalyst, utilizing cost-effective bases such as KOH, *t*-BuOK, and K_2CO_3, resulting in **22** and **23** compounds with excellent yields (Scheme 4).[46]

A sulfur-based catalyst was shown to efficiently produce benzimidazole derivatives according to Nguyen *et al.* The reaction initiates with 1,2-dibenzyldisulfane **24** and *O*-phenylenediamine derivative **25** in *N*-methyl-2-pyrrolidone (NMP) and DMSO at 100 °C to obtain benzimidazole derivative **26**.[47] Moreover, in the same year, Nguyen reported a multi-component one-pot synthesis using maleic anhydride **28**, benzyl amine **27**, and *O*-phenylenediamine **14**, which undergo

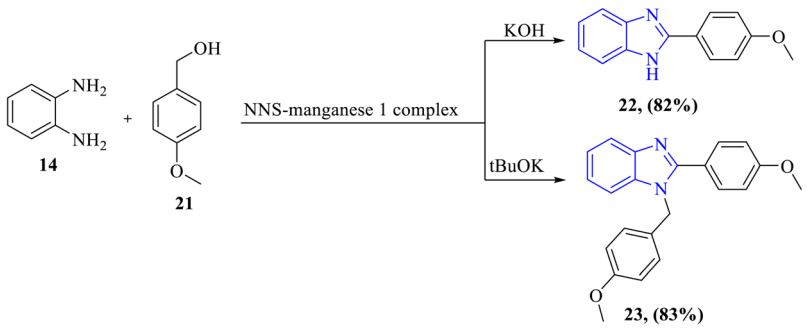

Scheme 4 Manganese(I)-catalyzed synthesis of benzimidazoles **22** and **23** from aromatic diamines **14** and primary alcohols **21** using a phosphine-free NNS–Mn complex.

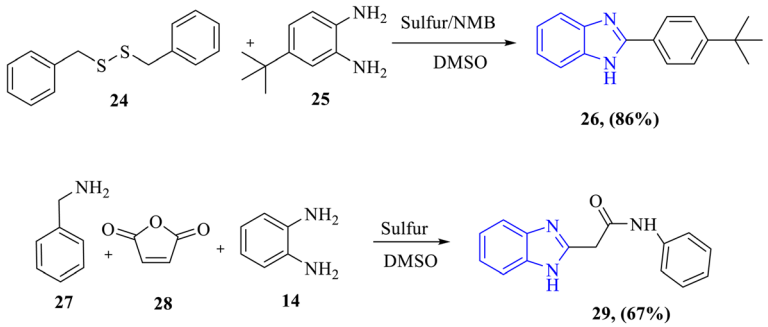

Scheme 5 Sulfur-catalyzed synthesis of benzimidazole **26** from 1,2-dibenzyldisulfane **24** and *O*-phenylenediamine derivative **25** in NMP/DMSO at 100 °C. One-pot, multi-component synthesis of benzimidazole **29** from benzylamine **27**, maleic anhydride **28**, and *O*-phenylenediamine **14** using a sulfur catalyst and DMSO as an oxidant.

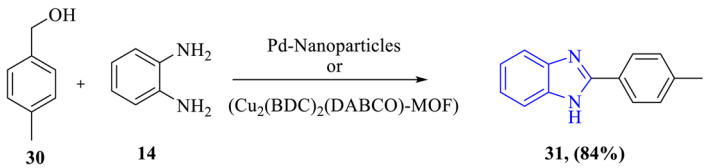

Scheme 6 Copper-palladium-catalyzed solvent-free synthesis of benzimidazole **31** from benzyl alcohol **30** and *O*-phenylenediamine **14** *via* dehydrogenative coupling.

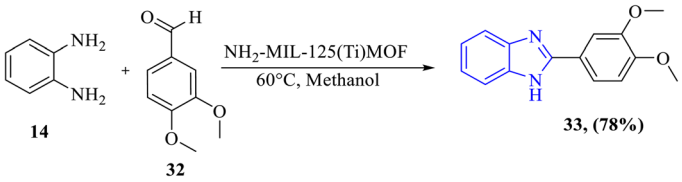

Scheme 7 MOF-catalyzed oxidative cyclization of *O*-phenylenediamine **14** with 3,4-dimethoxybenzaldehyde **32** for the rapid synthesis of benzimidazole **33**.

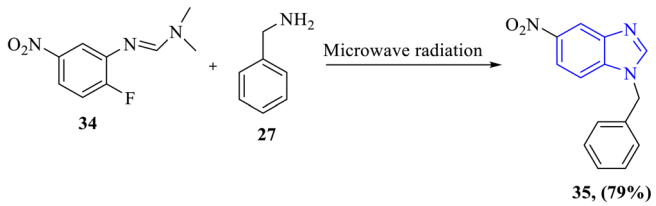

Scheme 8 Metal-free microwave-assisted synthesis of N-substituted benzimidazole **35** from a fluoro-aryl formamidine **34** and a primary amine derivative **27**.

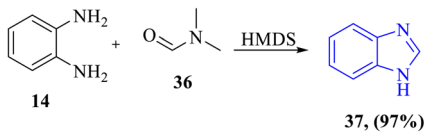

Scheme 9 Metal-free synthesis of benzimidazole (**37**) from *O*-phenylenediamine **14** and DMF **36** using hexamethyldisilazane (HMDS).

oxidation, decarboxylation, and cyclization to form a benzimidazole product **29**. In this reaction, sulfur functions as a catalyst, while DMSO serves as an oxidizing agent, resulting in a substantial yield of the benzimidazole scaffold (Scheme 5).[48]

Using a copper–palladium catalyst significantly improved the efficacy of the reaction between benzyl alcohol **30** and *O*-phenylenediamine **14** in the synthesis of benzimidazole **31**, as illustrated by Mokhtari, which underwent a dehydrogenative coupling reaction as a novel catalyst under solvent-free conditions. The catalyst employed in this reaction is reusable (Scheme 6).[49]

The research conducted by Sankar and his team in 2020 reported expeditious synthesis of benzimidazole **33** by the reaction of *O*-phenylenediamine **14** *via* oxidative cyclization using a metal–organic framework (MFO) as an efficient catalyst, as it increases the electrophilicity of 3,4-dimethoxybenzaldehyde **32** and enhances the rate of the reaction resulting in high yields with short time of the reaction (Scheme 7).[50]

1.2.3 Metal-free benzimidazole synthesis. Metal-free synthesis of benzimidazoles has emerged as a sustainable and environmentally friendly alternative to traditional metal-catalyzed methods. These approaches align with the principles of green chemistry, avoiding the use of expensive, toxic, or scarce metal catalysts, and often operate under mild conditions with high yields.[26,51,52] In 2019, Liu *et al.* presented a metal-free method for the synthesis of *N*-substituted benzimidazole **35** with microwave radiation. The reaction between fluoro-aryl formamidines **34** and derivatives of primary amines **27** gives high yields (Scheme 8).[53]

A metal-free reaction including a simple reagent was performed by Mostafavi *et al.* for the synthesis of **37**. In this reaction, *O*-phenylenediamine **14** and DMF **36** converted into benzimidazole using hexamethyldisilazane (HMDS) as a reagent. This reaction is free of any acid, transition metal, or solvent, yet it produces a great yield (Scheme 9).[54]

The one-step reaction approach for the synthesis of benzimidazole was demonstrated by Feizpour *et al.*, utilizing a cobalt ascorbic acid complex coated on TiO_2 nanoparticles to synthesize benzimidazoles **42** that, upon exposure to intermediate **41**, underwent aerobic photooxidative cyclization reaction to offer the target compound **42**. The catalyst in this reaction is reusable, and the process is conducted by photocatalysis-based organic synthesis (Scheme 10).[55]

A sustainable approach for synthesizing benzimidazole **44** was developed by Gan *et al.* using the *O*-phenylenediamine derivative **43**, in which it was condensed with dimethylformamide and its derivatives. In this approach, an imidazolium hydrochloride salt serves as the chemical initiator and activates formamide (Scheme 11).[56]

1.2.4 Green synthesis of benzimidazole. The green synthesis of benzimidazoles has emerged as a focal point in medicinal chemistry, aligning with the principles of sustainability, environmental responsibility, and energy efficiency.

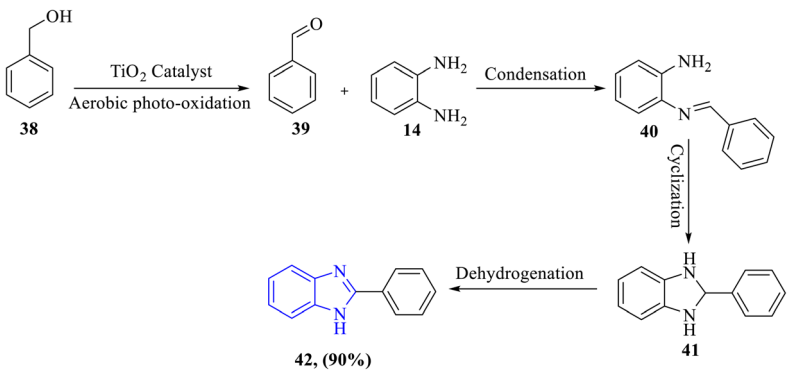

Scheme 10 Photocatalytic one-step synthesis of benzimidazoles **42** *via* aerobic photooxidative cyclization of intermediate **41** using a cobalt ascorbate-TiO_2 nanoparticle catalyst.

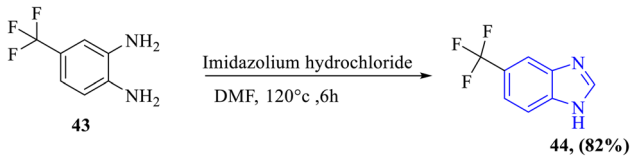

Scheme 11 Sustainable synthesis of benzimidazole **44** *via* the condensation of *O*-phenylenediamine derivative **43** with dimethylformamide using imidazolium hydrochloride salt as an initiator.

Recent advancements in this area emphasize the use of eco-friendly reagents, renewable resources, and energy-saving methodologies, reducing the environmental footprint while maintaining high synthetic efficiency.[57–60]

A novel, environmentally friendly method for the synthesis of benzimidazole **46** was reported by Arya *et al. via* one-pot route synthesis of 2-nitroaniline **45** using novel silver nanoparticles from green algae as a catalytic agent, resulting in its reduced form **14** that reacts with appropriate aldehyde **49**. Interestingly, it produced a high yield product (Scheme 12).[61]

The work by Di Gioia *et al.* in 2019 presented a method for the synthesis of benzimidazole scaffolds **50** and **51** *via* the reaction of *O*-phenylenediamine **14** with appropriate aldehydes **48** and **49** using Deep Eutectic Solvents (DESs) such as choline chloride **47**, as it serves as a medium and reagent at the same time. It provides advantages concerning the yield regarding compound **50**. Furthermore, the reaction with two molar amounts of aldehydes containing electron-withdrawing groups (as 2,4-dichlorobenzaldehyde) might occur owing to the electron-deficient aldehydes having a lower density of negative charge on the oxygen atom of the carbonyl group. Hence, they do not simply coordinate with the DES components, leading to the hydrogen bonding interaction, and therefore, the formation of the disubstituted product **51** is not favored (Scheme 13).[62]

In their research published in 2021, Thakore and his team reported the synthesis of polymer vesicles loaded with copper nanoparticles (CuNPs@vesicles) functioning as nanoreactors. These nanoreactors were utilized for the production of 2-substituted benzimidazole **53** in one-pot synthesis. The CuNPs@vesicles converted 2-nitroaniline into *O*-phenylenediamine **14**, which subsequently serves as a precursor for the production of benzimidazole. The authors also investigated the impact of substituents on aldehydes. Thus, aldehydes substituted with electron-withdrawing groups (EWG) as **52** need shorter reaction times than those substituted with electron-releasing groups (ERG). The complete series of reactions occurs in an aqueous medium under ambient circumstances (Scheme 14).[63]

1.2.5 Photo-catalyzed reaction. Photo-catalyzed reactions have gained significant attention as innovative and sustainable approaches for synthesizing benzimidazole derivatives. Leveraging light energy to drive chemical transformations, these methodologies align with green chemistry principles, offering high efficiency, mild reaction conditions, and reduced environmental impact. This section highlights the recent advancements in photo-catalyzed strategies for benzimidazole synthesis.[64–66]

In a study published in 2021, Montini *et al.* reported the synthesis of benzimidazole *via* a one-pot process through

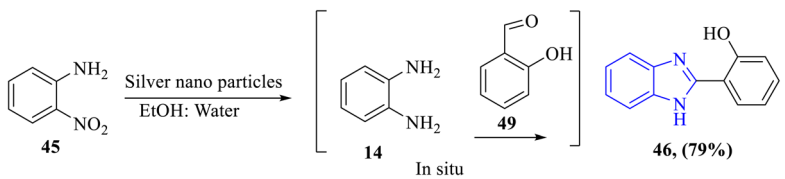

Scheme 12 Green one-pot synthesis of benzimidazole **46** *via* silver nanoparticle-catalyzed reduction of 2-nitroaniline **45** to *O*-phenylenediamine **14**, followed by reaction with aldehyde **49**.

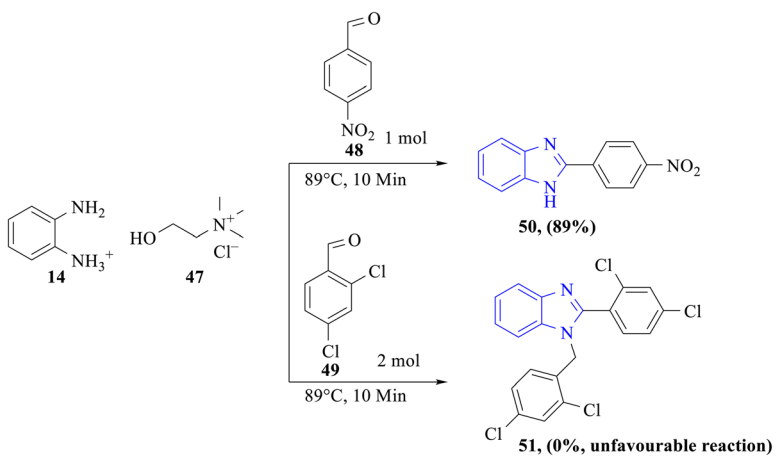

Scheme 13 Synthesis of benzimidazole **50** from *O*-phenylenediamine **14** and aldehyde **48** using deep eutectic solvents (choline chloride **47** serving as both the medium and the reagent).

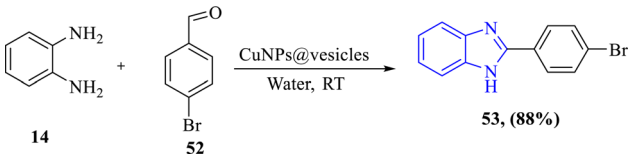

Scheme 14 One-pot synthesis of 2-substituted benzimidazole **53** using CuNPs@vesicle nanoreactors, converting 2-nitroaniline into *O*-phenylenediamine **14**, followed by reaction with substituted aldehydes **52** in an aqueous medium.

irradiation of dinitrobenzene **54** in 96% ethanol using Pt/TiO_2–B, N as a photocatalyst, where the molar level of dinitrobenzene gradually reduced with total conversion achieved after approximately 17 hours. Throughout that time, the molar proportion of nitroaniline **45** increased rapidly within the first 2 hours, exceeding 30–40%, and remained within this range until the complete consumption of dinitrobenzene; subsequently, the quantity of nitroaniline decreased as it was reduced and transformed into *O*-phenylenediamine **14** that reacted with appropriate aldehyde **55** resulting in benzimidazole product **56** (Scheme 15).[67]

The photocatalytic properties of cobalt-loaded titanium dioxide (Co–TiO_2) under solar light exposure, as shown by Kumaraswamy *et al.* in 2022, reported an eco-friendly approach for the synthesis of 2-aryl benzimidazoles **58**, where the Co–TiO_2 photocatalysts exhibited superior catalytic performance relative to pure TiO_2 attributed to greater charge separation and visible-light activity. The synthesis procedure performed with renewable solar energy produced good yields up to 85% with optimized 2% Co–TiO_2 catalysts *via* a reaction with *O*-phenylenediamine **14** with primary alcohol furan-2-ylmethanol **57**. This method provides the concepts of green chemistry (Scheme 16).[68]

The 2023 research by Abdelhamid *et al.* developed the synthesis of benzimidazole **60** by the reaction of *O*-phenylenediamine **14** with suitable aldehyde **59** utilizing a solid-state acid composed of zirconium oxosulfate embedded into carbon ($ZrOSO_4$@C) in a single vessel as a catalyst allowing condensation and cyclization under light radiation at room temperature which resulted in high yields and purity (Scheme 17).[69]

1.2.6 Efficient synthetic routes for benzimidazole-based compounds. The synthesis of benzimidazole-based scaffolds has developed through different efficient strategies depending on the desired product and reaction conditions. Traditional methods including cyclocondensation of *O*-phenylenediamines with carboxylic acids, esters, or aldehydes remain highly efficient and widely used due to their simplicity and good

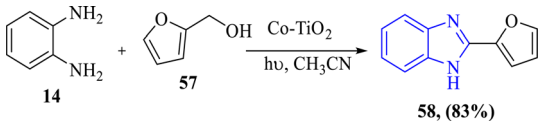

Scheme 16 Solar-light-driven synthesis of 2-aryl benzimidazole **58** from *O*-phenylenediamine **14** and furan-2-ylmethanol **57** using a cobalt-loaded TiO_2 (Co–TiO_2) photocatalyst.

Scheme 17 Room-temperature light-assisted synthesis of benzimidazole **60** from *O*-phenylenediamine **14** and aldehyde **59** catalyzed using solid-state $ZrOSO_4$@C acid.

yields.[39,44] Furthermore, metal-catalyzed reactions such as copper- or palladium-mediated oxidative cyclization are particularly significant for synthesizing benzimidazole derivatives.[46] Moreover, metal-free approaches are gaining attention for their lower toxicity especially in pharmaceutical applications where metal residues are undesirable.[56] Green synthesis protocols, employing water and Deep Eutectic Solvents (DESs), often under solvent-free or microwave-assisted conditions, offer reduced reaction times and cleaner profiles.[62] Finally, emerging photo-catalyzed methods using visible light activation have opened new avenues for environmentally sustainable benzimidazole synthesis under mild conditions without harsh reagents.[67] In parallel, green synthetic strategies are increasingly recognized for their efficiency and compatibility with green chemistry principles. Taken together, these two approaches are distinguished as the most efficient and practical for the synthesis of benzimidazole scaffolds, offering a balance of accessibility and sustainability that aligns well with the current demands of medicinal and organic chemistry research.

1.2.7 Toxicological considerations and structural optimization in benzimidazole-based compounds. Evaluating the toxicity of benzimidazole-based compounds is essential during the early stages of their drug development, particularly due to their structural similarity to purine bases like adenine and guanine.[70] Several benzimidazole derivatives reviewed here, such as those containing triazole, azomethine, or metal-coordinating groups, exhibit promising antimicrobial activities with favorable safety profiles, as evidenced by *in vitro* cytotoxicity data and

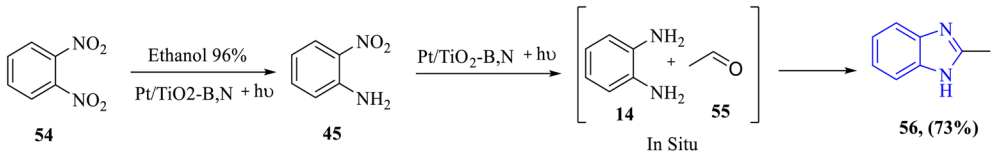

Scheme 15 One-pot synthesis of benzimidazole **56** *via* photocatalytic reduction of dinitrobenzene (**54**) to *O*-phenylenediamine **14** followed by condensation with aldehyde **55** using a Pt/TiO_2–B,N catalyst in ethanol.

brine shrimp assays. Planar aromaticity, the presence of reactive functional groups such as aldehydes, and the ability of a molecule to chelate metal ions are known as structural features that may contribute to toxicity through off-target binding.[71,72] To control toxicological liabilities, the rational design that includes minimizing lipophilicity may reduce nonspecific binding and ensure metabolic stability to prevent bioactivation into toxic intermediates. Furthermore, compounds such as Ni(II) complexes suggest that controlled coordination chemistry can enhance safety as mentioned before for compound **61a**.[73] Hence, future benzimidazole derivatives should be optimized not only for their potency but also for their ADMET properties. This can be achieved through *in silico* prediction tools and preliminary evaluations that aimed to minimize mutagenicity, carcinogenicity, and organ-specific toxicity.

1.2.8 Evaluation of nitrosamine risk in benzimidazole-based scaffolds. While benzimidazole-based scaffolds are generally not classified as high-risk frameworks for nitrosamine formation, it is important to assess the structural features of synthesized derivatives for potential risk. In the present review, the majority of the synthesized compounds including Schiff bases, triazole hybrids, and metal complexes do not possess secondary or tertiary amines directly attached to the benzimidazole core that were regularly linked in nitrosamine formation. However, a few compounds such as those featuring *N*-alkylated benzimidazoles may contain nitrosamine precursors, particularly if exposed to nitrosating agents under acidic conditions during synthesis. Furthermore, synthetic routes that include formamidine intermediates, DMF, or dimethylamine derivatives may theoretically introduce trace nitrosamine risk.[74] To date, nitrosamine risk assessments are not reported for benzimidazole derivatives at the discovery stage, but considering their increasing regulatory importance, especially FDA, such evaluations should become a routine component of early-stage drug development. Rational design strategies aimed to minimize the risk of nitrosatable amines, substituting with safer reagents and monitoring residual solvents. Collectively, future studies on benzimidazole-based compounds should integrate predictive nitrosamine risk models.

2 Pharmacological activities

2.1 Antibacterial activities

Due to the isosteric nature of benzimidazole and its derivatives with purine molecules, a competitive interaction occurs, leading to the inhibition of nucleic acid synthesis, which results in cell damage and cell death. Additionally, it has been noted that some benzimidazole compounds have the ability to interfere with the process of folate biosynthesis in microbial cells, thus blocking the formation of folates resulting in the inhibition of bacterial growth. Mahmood *et al.* designed and synthesized benzimidazole derivatives containing metals incorporated with an azomethine group, leading to the formation of complexes, which seem to be responsible for various biological activities with high safety margin. Their mode of action depends on binding to DNA. thus preventing the replication process of genetic materials. Compounds **61a–c** were investigated against one Gram-positive bacterial strain *Micrococcus luteus* and one Gram-negative strain *Escherichia coli* (Fig. 4). Compound **61a** displayed outstanding antibacterial activities with effective inhibition zone diameters (DIZ = 16.8 mm and 18.8 mm) comparable to the inhibition zone diameter values of the reference drug kanamycin (DIZ = 24.6 mm and 21.2 mm), against *M. luteus* and *E. coli*, respectively. Furthermore, compounds **61b** and **61c** containing other metals, such as Zn and Cu, exhibited activity only against *E. coli* (DIZ = 18.9 mm and 11.8 mm, respectively) (Table 1). The results were confirmed through the inhibition of DNA gyrase *via* binding activity by a thermal denaturation test, and as the temperature of the double-stranded DNA solution increases, the double helix undergoes denaturation due to the dissociation of hydrogen bonds between the base pairs. Therefore, it can be concluded that the Ni complex is a strong DNA binder due to its high lipophilicity increasing penetration through lipid membranes, facilitating the interaction with DNA by intercalation; then, the Cu complex is the weakest DNA binder, representing an advantage in terms of safety, as the Ni complex displayed no toxicity in the brine shrimp assay, with the exception of the Cu complex which showed slight toxicity.[73]

Dokla and collaborators designed and synthesized *N*-alkyl-2-substituted-1*H*-benzimidazole derivatives **62a–d** and evaluated their activity against one bacterial strain *E. coli* (TolC mutant strain) (Fig. 5), as well as the presence of an outer membrane in most Gram-negative bacteria imparts an additional barrier against the penetration of many antibiotics. Efflux pumps might also be a reason for the lack of antimicrobial activity; hence, designated compounds were co-administrated with colistin (membrane disrupting antibiotic) to detect if the outer membrane impedes the antibacterial activity of the synthesized compounds. Compound **62a** was the derivative with the best activity against *E. coli* (MIC = 2 μg mL^{-1}) compared to the reference linezolid (MIC = 8 μg mL^{-1}). Moreover, compounds **62b** and **62c** displayed good activity (MIC = 16 μg mL^{-1}). However, compounds **62d** and **62e** exhibited weak activity against *E. coli* (MIC values > 128 μg mL^{-1}) (Table 2). Moreover, compound **62a** represents an excellent safety profile against human colorectal (Caco-2) and monkey kidney epithelial cells. Structure activity relationship (SAR) revealed that according to

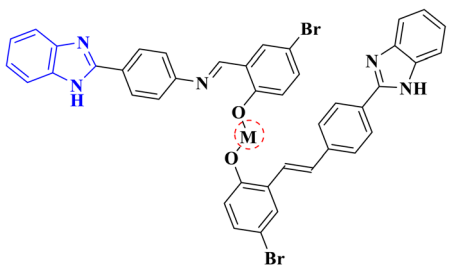

61a-c

61a: M= Ni, (60%)
61b: M= Zn, (73%)
61c: M= Cu, (80%)

Fig. 4 Chemical structures of metal-complexed benzimidazole derivatives **61a–c** evaluated for antibacterial activity.

Table 1 Antibacterial activity diameter inhibition zones of compounds **61a–c** compared to kanamycin against *Micrococcus luteus* and *Escherichia coli*

	Diameter inhibition zone (mm)	
Compound	*M. luteus*	*E. coli*
61a	16.8	18.8
61b	11	18.9
61c	14.9	11.8
Kanamycin	6.8	8.4

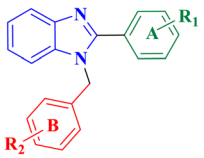

62a-e

62a: R^1=3-$NHSO_2CH_3$, R^2= 4-CH_3, (37%)
62b: R^1=3-$NHSO_2CH_3$, R^2= H, (21%)
62c: R^1=3-CN, R^2= 4-CH_3, (20%)
62d: R^1=4-OCH_3, R^2= 4-CH_3, (28%)
62e: R^1=3-$NHSO_2CH_3$, R^2= 3-CN, (48%)

Fig. 5 *N*-alkyl-2-substituted benzimidazoles **62a–e** evaluated with colistin for enhanced Gram-negative activity.

ring A introduction substituents at *meta* position give excellent antimicrobial activity **62a–c** also 3-$NHSO_2CH_3$ group is optimal for activity while substitution at *para* positions diminished antibacterial activity as compound **62d**. Furthermore, ring B substitution at *para* position gives outstanding antimicrobial activity to **62c** compared to *meta* substituents **62e**.[75]

In 2018, Bistrović and colleagues designed novel scaffolds of benzimidazole derivatives by variation in positioning 2,5 with phenyl substituents on the triazole ring, and the amidino moieties allowed the development of compounds with comparable activity as an antibacterial agent. Compounds

Table 2 Minimum inhibitory concentrations (MIC) of compounds **62a–e** against *E. coli* (TolC mutant strain) in the presence of colistin, with comparison to linezolid

	Minimum inhibition concentration (μg mL^{-1})
Compound	*E. coli*
62a	2
62b	16
62c	16
62d	>128
62e	>128
Linezolid	8

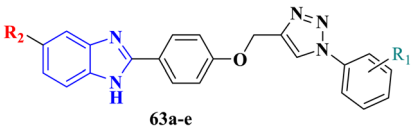

63a-e

63a: R^1= H , R^2= , (58%)
63b: R^1= 4-OCH_3 , R^2= , (53%)
63c: R^1= 2, Cl , R^2= , (28%)
63d: R^1= H , R^2= , (30%)
63e: R^1= 4-OCH_3 , R^2= , (70%)

Fig. 6 Structures of benzimidazole–triazole hybrids with amidino moieties **63a–e**, synthesized for evaluation against Gram-positive and Gram-negative bacteria.

63a–e were investigated against two Gram-positive bacterial strains, namely, *Methicillin-resistant Staphylococcus aureus* (*MRSA*) and *E. faecalis*, and three Gram-negative bacteria, namely, *E. coli*, *K. pneumoniae* and *P. aeruginosa* (Fig. 6). Compounds **63a** displayed broad-spectrum antibacterial activities against *MRSA* and *E. faecalis* (MIC = 16 μg mL^{-1} and 32 μg mL^{-1} respectively), comparable to the MIC value of the reference drug ampicillin (4 μg mL^{-1} and 1 μg mL^{-1}, respectively) and excellent activity against *E. coli* and *K. pneumoniae* with MIC values of 4 μg mL^{-1} and 8 μg mL^{-1}, respectively, in comparison with the MIC value of the reference drug ceftazidime (8 μg mL^{-1} and >128 μg mL^{-1}) with high affinity to DNA presenting high potency against extended-spectrum β-lactamase (ESBL)-producing *E. coli* and *K. pneumoniae*. Compound **63c** exhibited greater antibacterial activity against only Gram-positive bacterial strains than compound **63a** with MIC values of 8 μg mL^{-1} and 32 μg mL^{-1} with respect to the reference drug ampicillin. Furthermore, compounds **63d** and **63e** demonstrated less antibacterial activity only against Gram-positive bacteria with MIC values ranging from 128 μg mL^{-1} to 256 μg mL^{-1}, while compound **63b** showed no activity against all bacterial strains (Table 3). Furthermore, the active compounds still had less antibacterial activities than ampicillin, which might be due to irreversible binding in cell wall biosynthesis. In contrast, the designated compounds have alternative modes of action, including DNA interaction and potential membrane disruption, which are inherently less potent in the initial stages of development. These findings support the need for future studies focused on optimizing triazole substitution patterns or combining these compounds with ampicillin to enhance antibacterial efficacy through dual mechanisms.

Table 3 MIC values of benzimidazole–triazole derivatives **63a–e** against Gram-positive and Gram-negative bacterial strains, against ampicillin and ceftazidime

	Minimum inhibition concentration (μg mL^{-1})			
Compound	*MRSA*	*E. faecium*	*E. coli*	*K. pneumoniae*
63a	16	32	4	8
63b	—	256	—	—
63c	8	32	—	—
63d	128	128	—	—
63e	256	256	—	—
Ampicillin	4	1	—	—
Ceftazidime	—	—	8	>128

According to SAR evaluations, it was observed that the type of amidino moiety had positive impact one the activity in case of no substitution gave wide spectrum compound **63a** on both Gram-positive and Gram-negative bacteria while the lipophilic character of isopropyl and chloro substitutions increased Gram-positive selectivity, especially against MRSA strain **63c** while introduction of bulky methoxy group at *para* position revealed diminished or no antibacterial against all tested strains **63b** and **63e**.[76]

In 2021, Rashdan *et al.*, reported that benzimidazole derivatives **64a–c** (Fig. 7) induced highly expected antimicrobial activity through inhibition DNA gyrase subunit B leading to disruption of DNA synthesis, subsequently, cell death. DNA gyrase is considered as an essential bacterial enzyme that is included in the control of topological transitions of DNA, therefore the enzyme has been selected as a therapeutic target for many antimicrobial agents. Compounds were screened against one Gram-positive bacteria, *S. aureus*, and two Gram-negative bacteria, *E. coli* and *P. aeruginosa*, to evaluate their antibacterial efficacy. Compounds **64a** and **64b** exhibited excellent antibacterial activity against *S. aureus*, *E. coli* and *P. aeruginosa* with an inhibition zone diameter ranging from 17 mm to 29 mm compared to that of the reference drug ciprofloxacin (20 mm, 23 mm and 21 mm, respectively). Furthermore, compound **64c** showed good antibacterial activity

Table 4 Diameter inhibition zone of compounds **64a–c** against *S. aureus*, *E. coli*, and *P. aeruginosa*, compared to ciprofloxacin

	Diameter inhibition zone (mm)		
Compound	*S. aureus*	*E. coli*	*P. aeruginosa*
64a	24	25	17
64b	29	21	19
64c	23	—	13
Ciprofloxacin	20	23	21

against *S. aureus* with an inhibition zone diameter of 23 mm and moderate activity against *P. aeruginosa* with an inhibition zone diameter of 13 mm with respect to the inhibition zone diameter of the control drug ciprofloxacin of 20 mm and 21 mm, respectively (Table 4). Moreover, it did not prove any activity against *E. coli*. Moreover, molecular docking studies for designated compounds **64a** and **64b** displayed similar binding modes towards the targeted enzyme DNA gyrase B as the co-crystallized ligand ciprofloxacin with Thr165. The SAR findings suggested that the presence of chlorine atom in the phenyl ring at position-4 in derivative **64b** was favorable, also existence of thiadiazole ring **64a** and **64b** essential for activity and give antibacterial action against all tested strains thus could be illustrated in compound **64c**.[77]

Deswal and his team designed a novel series of benzimidazole-1,2,3-triazole-indoline derivatives exemplified by **65a–b** using a click reaction (Fig. 8). Compounds were screened against two bacterial strains to evaluate their activity: one Gram-negative bacteria, *E. coli*, and one Gram positive bacteria *S. aureus*. They displayed significant antibacterial activity. Compound **65a** showed excellent activity against *E. coli* and *S. aureus* with MIC values of 0.026 μg mL^{-1} and 0.031 μg mL^{-1}, respectively, compared to the control drug norfloxacin with MIC values of 0.039 and 0.020 μg mL^{-1}, whereas Compound **65b** exhibited excellent activity against *E. coli* and good activity against *S. aureus* with MIC values of 0.030 μg mL^{-1} and 0.060 μg mL^{-1}, respectively, comparable to the MIC reference drug norfloxacin (Table 5). The notable broad-spectrum antibacterial activity of the compounds particularly **65a** proved to be

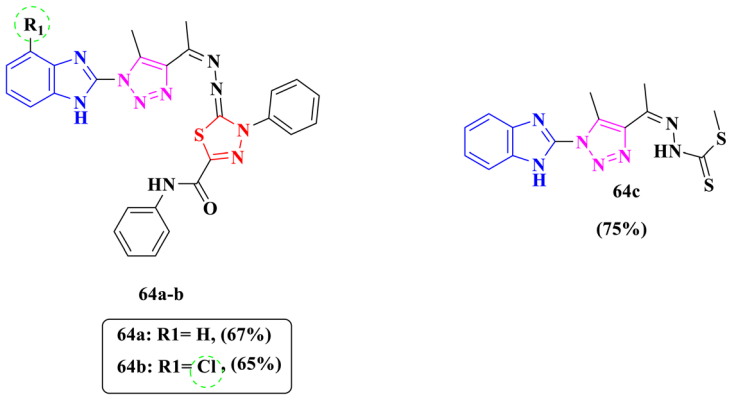

Fig. 7 Benzimidazole-based compounds **64a–c** developed as antibacterial agents targeting the DNA gyrase B subunit.

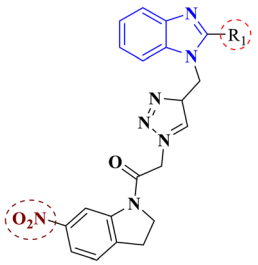

65a-b

65a: R1: -C_6H_5N, (70%)
65b: R1: -CH_3, (86%)

Fig. 8 Benzimidazole–triazole–indoline hybrids **65a–b** designed as antibacterial agents against *E. coli* and *S. aureus*.

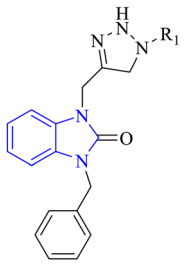

66a-c

66a: R1= -CH_2COOEt, (67%)
66b: R1= -CH_2Ph, (68%)
66c: R1= -$(CH_2)_{11}CH_3$, (89%)

Fig. 9 Benzimidazole–triazole hybrids **66a–c** tested against *S. aureus*, *E. coli*, and *P. aeruginosa*.

associated with the presence of a hydrophilic moiety as the pyridine ring at position 2 of the benzimidazole nucleus and typically electron-withdrawing group, as (NO_2) on the indole moiety was optimal for activity. However, the presence of a lipophilic moiety as the methyl group proved to be selective against *E. coli* **65b**.[78]

The research by Saber *et al.* proved that a 1,2,3-triazole moiety could serve as a linker connected to the benzimidazole *via* a cycloaddition reaction. This parameter plays an essential role in membrane permeation into the microbial cell, and the resulting bio isosteric effects on peptide linkage through hydrogen bond formation, dipole–dipole interaction and π stacking interactions led to high-affinity binding with biological targets increasing membrane permeation into the microbial cell. Moreover, the intermolecular interaction of the designated compounds was determined by Hirshfeld surface analyses; in addition, the Monte Carlo method was used to investigate the interfacial interaction of these derivatives with iron, copper and aluminum surfaces and provide better anti-corrosion properties for iron than copper and aluminum. Moreover, substitution on N_1 on the triazole moiety with aliphatic ester chain, compound **66a**, gave outstanding broad-spectrum antibacterial activities compared to substitution with the benzyl ring, compound **66b**, that had selectivity only against Gram-positive bacteria, while increasing the length of aliphatic chain abolished the antimicrobial activity of **66c**. Compounds **66a–c** were investigated for their antimicrobial activity against one Gram-positive bacteria, *S. aureus*, and two Gram-negative bacterial strains, *E. coli* and *P. aeruginosa* (Fig. 9). Compound **66a** exhibited greater antibacterial activity against *S. aureus* and *E. coli* with an equipotent MIC value of 3.12 μg mL^{-1} compared with the MIC value of the control drug chloramphenicol, 12.50 μg mL^{-1} and 6.25 μg mL^{-1}, respectively, while compound **66b** showed excellent activity particularly on *S. aureus* with an MIC value of 3.12 μg mL^{-1} and mild activity against *E. coli* with an MIC value of 25 μg mL^{-1}, comparable to the MIC value of the reference drug chloramphenicol. However, compound **66c** displayed weak antibacterial activity with MIC values of 25 μg mL^{-1}, 12.50 μg mL^{-1} and 25 μg mL^{-1} against *S. aureus*, *E. coli* and *P. aeruginosa*, respectively. Compounds **66a** and **66b** had less antibacterial action on *P. aeruginosa* with MIC values of 12.50 μg mL^{-1} and 25 μg mL^{-1}, respectively, compared to the MIC value of 6.25 μg mL^{-1} of the reference drug chloramphenicol (Table 6).[79]

Al-blewi and his team proved that antibacterial activity is affected by substitutions on the benzimidazole ring, while the antibacterial potency of the mono-substituted benzimidazole **67a** was found to be less than that of the di-substituted benzimidazole **67b–c**, which may be attributed to the synergistic effect between the benzimidazole and sulfonamoyl nucleus and the enhanced lipophilicity of the bis-substituted derivatives that positively affects the activity against Gram-negative tested strains. Compounds **67a–c** were investigated for their

Table 5 MIC values of **65a–b** against *E. coli* and *S. aureus* compared to norfloxacin

	Minimum inhibition concentration (μg mL^{-1})	
Compound	*E. coli*	*S. aureus*
65a	0.026	0.031
65b	0.030	0.060
Norfloxacin	0.039	0.020

Table 6 Minimum inhibitory concentrations (MIC, μg mL^{-1}) of compounds **66a–c** against *S. aureus*, *E. coli*, and *P. aeruginosa*, compared with chloramphenicol

	Minimum inhibition concentration (μg mL^{-1})		
Compound	*S. aureus*	*E. coli*	*P. aeruginosa*
66a	3.125	3.125	12.5
66b	3.125	25	12.5
66c	25	12.5	25
Chloramphenicol	12.5	6.25	6.25

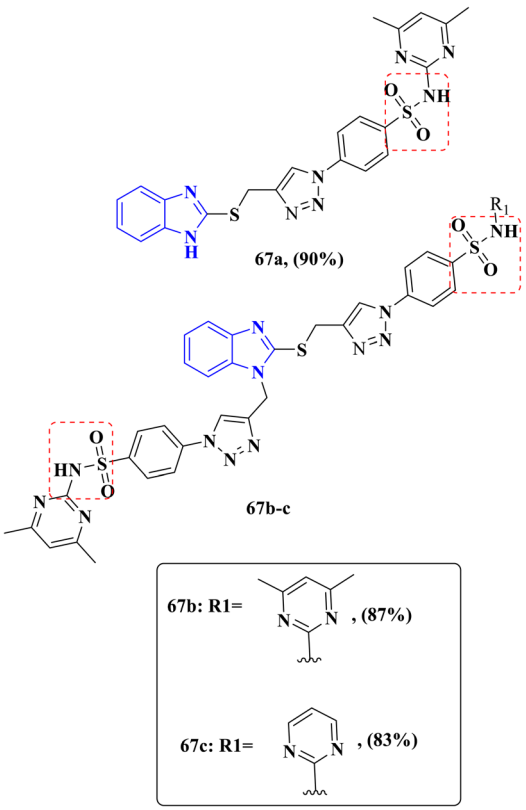

Fig. 10 Antibacterial benzimidazole derivatives **67a–c** evaluated against Gram-positive and Gram-negative strains.

antimicrobial activity against two Gram-positive bacteria, *Bacillus cereus* and *S. aureus*, and two Gram-negative bacterial strains, *E. coli* and *P. aeruginosa* (Fig. 10). Compound **67b** showed outstanding antibacterial activity against all the tested bacterial strains with an equipotent MIC value of 32 μg mL^{-1} against *B. cereus and S. aureus* comparable to the MIC value of the reference drug ciprofloxacin 8 μg mL^{-1} and 4 μg mL^{-1}, respectively, and an equipotent MIC value of 64 μg mL^{-1} against *E. coli* and *P. aeruginosa* in comparison with the MIC value of ciprofloxacin 8 μg mL^{-1} and 4 μg mL^{-1}, respectively. Moreover, derivative **67c** displayed good antibacterial activity against all tested strains with an equipotent MIC value of 64 μg mL^{-1}. Furthermore, compound **67a** exhibited less antibacterial properties against *B. cereus* and *S. aureus* strains with an equal MIC value of 64 μg mL^{-1} comparable to the control drug

Table 7 MIC values of compounds **67a–c** against four bacterial strains, benchmarked with ciprofloxacin

	Minimum inhibition concentration (μg mL^{-1})			
Compound	*B. cerus*	*S. aureus*	*E. coli*	*P. aeruginosa*
67a	64	64	128	256
67b	32	32	64	64
67c	64	64	64	64
Ciprofloxacin	8	4	4	8

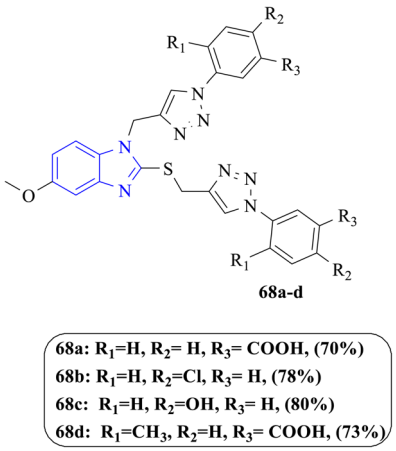

Fig. 11 4-Methoxybenzimidazole derivatives **68a–d** synthesized for bacterial evaluation against *S. aureus* and *E. coli*.

ciprofloxacin and against *E. coli* and *P. aeruginosa* with MIC values of 256 μg mL^{-1} and 128 μg mL^{-1}, respectively, with respect to the MIC value of the control drug ciprofloxacin (Table 7). Toxicity results for both compounds displayed good safety margin with neither carcinogenicity nor mutagenicity. In addition, *in silico* ADMET evaluation of the designated compound **67b** meets the criteria of drug-likeness and obeys Lipinski's rule of five, presenting a good candidate of further research and development.[80]

The study by Aparna and collaborators utilized similar techniques to obtain novel 4-methoxybenzimidazole derivatives **68a–d** (Fig. 11). The SAR study revealed that the synthesized compounds exhibited good antibacterial activity with MIC values of 58.78 μg mL^{-1} to 130.28 μg mL^{-1} in comparison with the reference drug ciprofloxacin 10 μg mL^{-1}. All the derivatives showed higher selectivity against Gram-positive strains than against Gram-negative strains except in derivative **68b** that had selectivity toward *E. coli* and the activity was provided by shifting in positioning on the phenyl ring attributed to the triazole moiety, through its incorporation with an atom of large radius as the chlorine group at position-4. Moreover, compound **68a** exhibited the highest potency against *S. aureus* and *E. coli*, attributed to hydrophilic substituents, as the carboxylic acid group at position 3 and the methyl substitution at the benzoic ring affected the potency negatively. Compound **68a** showed significant antibacterial activity against Gram-positive bacteria *S. aureus* with an MIC value of 58.78 μg mL^{-1} and mild activity against Gram-negative bacteria *E. coli* with an MIC value of 68.74 μg mL^{-1}, comparable to the MIC value of 10 μg mL^{-1} of the reference drug ciprofloxacin. However, compounds **68b** and **68c** showed comparable activities against *S. aureus* and *E. coli* bacteria, where compound **68b** showed MIC values of 106.83 μg mL^{-1} and 91.45 μg mL^{-1} compared to the MIC value of the reference drug ciprofloxacin, respectively. Nevertheless, compound **68c** exhibited MIC values of 83.74 μg mL^{-1} and 118.46 μg mL^{-1}, when compared to the MIC value of the reference drug ciprofloxacin. Compound **68d** also demonstrated less antibacterial activity against both strains

Table 8 MIC data for **68a–d** against *S. aureus* and *E. coli*, using ciprofloxacin as a reference drug

	Minimum inhibition concentration (μmol mL^{-1})	
Compound	*S. aureus*	*E. coli*
68a	58.78	68.74
68b	106.86	91.45
68c	83.47	118.46
68d	130.28	140.26
Ciprofloxacin	10	10

Table 9 MIC activity values of compounds **69a–c** against *B. subtilis* and *Y. pseudotuberculosis* against ampicillin

	Minimum inhibition concentration (μg mL^{-1})	
Compound	*B. subtilis*	*Y. pseudotuberculosis*
69a	62.5	62.5
69b	62.5	250
69c	31.25	62.5
Ampicillin	100	100

S. aureus and *E. coli* with MIC values of 130.28 μg mL^{-1} and 140.26 μg mL^{-1}, respectively, when compared with the MIC value of the control drug ciprofloxacin (Table 8). Furthermore, molecular modelling studies for the designated compound **68a** revealed a moderate inhibitory activity of enol acyl carrier protein reductase (FabI) interactions with amino acid residues Phe96, Met99, Tyr147, Tyr157 and Met160.[81]

The antibacterial properties of some benzimidazole derivatives **69a–c** were investigated by Kantar *et al.* against one Gram-positive bacteria *B. subtilis* and one Gram-negative bacteria *Yersinia pseudotuberculosis* (Fig. 12). The antibacterial activity ranged from good to moderate. Compound **69a** exhibited broad-spectrum activities against both tested strains with equipotent MIC values of 62.5 μg mL^{-1} against the MIC value of the control drug ampicillin 100 μg mL^{-1}, while compound **69b** had high selective activity against *B. subtilis* with an MIC value of 62.5 μg mL^{-1} and intense activity against *Y. pseudotuberculosis* with an MIC value of 250 μg mL^{-1} with respect to the reference drug ampicillin; however, compound **69c** exhibited the highest potency (MIC = 31.25 μg mL^{-1} and 62.5 μg mL^{-1}) against *B. subtilis* and *Y. pseudotuberculosis*, respectively, compared to the drug ampicillin (Table 9), and this high potency is probably due to the combination of the benzimidazole nucleus and the 1,2,4-triazole ring.[82]

Nandwana *et al.* proved that polycyclic aromatic compounds **70a–d** offered highly active antibacterial properties (Fig. 13), where compound **70a** exhibited the highest potency that may be explained by hybridization between the benzimidazole nucleus, quinazoline and triazole ring than the other azole derivatives **70b–d**. Those compounds were investigated against two Gram-positive bacteria, *S. aureus* and *B. subtilis*, and three Gram-negative bacteria, *E. coli*, *Salmonella typhi* and *Pseudomonas putida*, where compound **70a** showed significant activity against *S. aureus* and *B. subtilis* with an equipotent MIC value of 8 μg mL^{-1} compared to the MIC value of 6.25 μg mL^{-1} of the reference drug ciprofloxacin and displayed a greater equal MIC activity value of 4 μg mL^{-1} against *P. putida* and *E. coli* compared to the MIC value of 6.25 μg mL^{-1} of the reference drug ciprofloxacin. Compound **70b** showed good antibacterial activity against *S. aureus* and *B. subtilis* with MIC values of >8 μg mL^{-1} and 8 μg mL^{-1}, respectively, and significant activity against *E. coli* and *P. putida* with MIC values of >8 μg mL^{-1} and 8 μg mL^{-1} when compared to the control drug ciprofloxacin. Furthermore, compound **70c** also showed moderate activity with an equipotency MIC value of 16 μg mL^{-1} against both Gram-positive strains and Gram-negative bacteria *E. coli* and *S. typhi* comparable to the MIC value of the reference drug ciprofloxacin 6.25 μg mL^{-1}. Compound **70d** showed less antibacterial activity against Gram-positive strains with equal MIC values of 64 μg mL^{-1} and > 2 μg mL^{-1} for both Gram-negative strains *E. coli* and *P. putida*, respectively, in comparison to ciprofloxacin (Table 10). Furthermore, compound **70a** modulated the biofilm formation through biocidal mechanism either by degradation of the extracellular matrix or weakened the biofilm, which is an extracellular substance providing high resistance to microbes against phagocytosis and other components of the body's defense system. In addition, the bactericidal assay of propidium

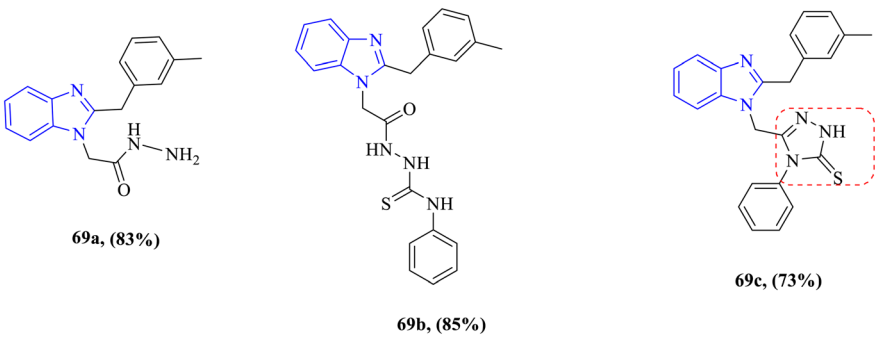

Fig. 12 Benzimidazole derivatives **69a–c** tested against *B. subtilis* and *Y. pseudotuberculosis*.

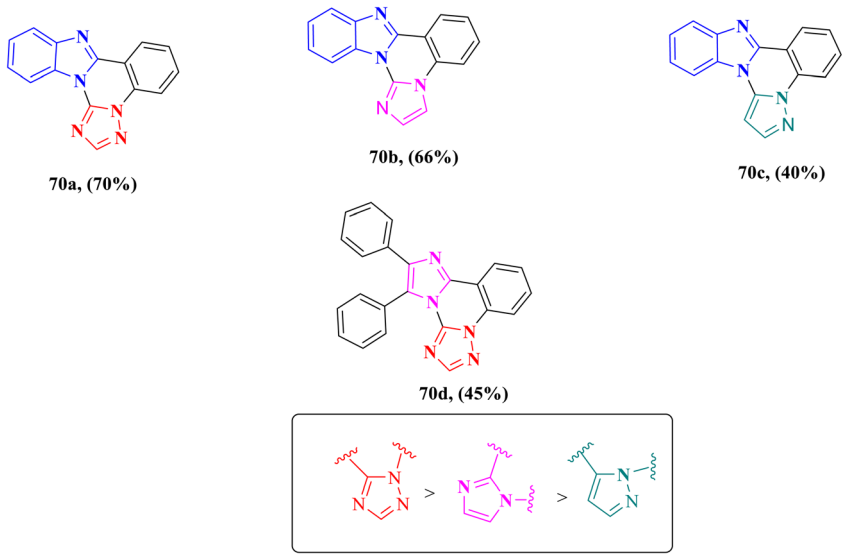

Fig. 13 Structures of polycyclic benzimidazole hybrids **70a–d** incorporating triazole and quinazoline moieties for antibacterial evaluation.

Table 10 MIC values of compounds **70a–d** against *S. aureus*, *B. subtilis*, *E. coli*, *P. putida*, and *S. typhi*, with ciprofloxacin as reference

	Minimum inhibition concentration (μg mL^{-1})			
Compound	*S. aureus*	*B. subtilis*	*P. putida*	*E. coli*
70a	8	8	4	4
70b	>8	8	8	>8
70c	16	16	16	16
70d	64	64	>32	>32
Ciprofloxacin	6.25	6.25	6.25	6.25

iodide and live-dead bacterial cell screening by using a mixture of acridine orange/ethidium bromide cause cell death, which might be due to considerable changes in the bacterial cell membrane. The synthesized compounds were also assessed for hemolytic activity, which indicated an acceptable standard towards human blood cells.[83]

The incorporation of 2-mercaptobenzimidazole with a 1,2,4-triazole moiety by Al-Majidi and colleagues yielded promising antibacterial compounds **71a–c** (Fig. 14). Compounds were evaluated for their antibacterial activity against Gram-positive bacteria *S. aureus* and Gram-negative bacteria *P. aeruginosa*. Compounds **71a** and **71b** displayed powerful activity against *S. aureus* with inhibition zone diameters of 18 mm and 19 mm when compared to the 33 mm of control drug amoxicillin, respectively, and moderate activity against *P. aeruginosa* with inhibition zone diameters of 14 mm and 11 mm when compared to the 32 mm of drug amoxicillin. Furthermore compound **71c** presented good activity against *S. aureus* with an inhibition zone diameter of 17 mm compared to the control drug amoxicillin; however, the activity against *P. aeruginosa* is a little effective, as indicated by an inhibition zone diameter of 15 mm compared to the antibiotic amoxicillin (Table 11).[84]

Research findings of Elgadil and his team proved that synthesized scaffolds of benzimidazole derivatives incorporated with a triazole ring induce antibacterial activity by inhibiting the activity of topoisomerase II (DNA gyrase), which is essential for bacterial cell survival. Compounds **72a–c** were investigated for their activity against one Gram-positive bacteria *S. aureus* and one Gram-negative bacteria *E. coli* (Fig. 15). Compound **72a** displayed greater activity against *S. aureus* than the reference drug ampicillin with an MIC value of 0.07 μm mL^{-1} comparable to 0.27 μm mL^{-1} and excellent activity against *E. coli* with an MIC value of 0.14 μm mL^{-1} when compared to the MIC value of the reference drug ampicillin 0.26 μm mL^{-1}. Moreover, compound **72b** exhibited

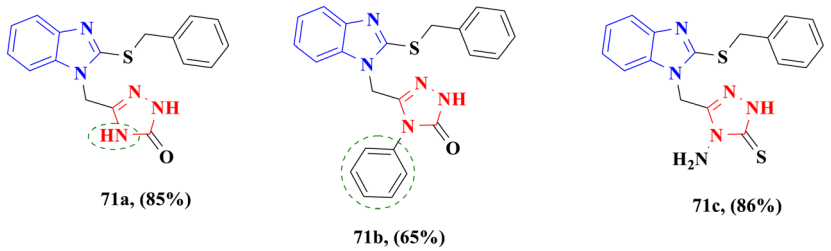

Fig. 14 2-Mercaptobenzimidazole–triazole derivatives **71a–c** tested against *S. aureus* and *P. aeruginosa*.

Table 11 Inhibition zone diameters of compounds **71a–c** against *S. aureus* and *P. aeruginosa*, compared with amoxicillin

	Diameter inhibition zone (mm)	
Compound	*S. aureus*	*P. aeruginosa*
71a	18	14
71b	19	11
71c	17	11
Amoxicillin	33	32

outstanding antibacterial activities against both bacterial strains with an equipotent MIC value of 0.14 μm mL^{-1} with respect to the MIC value of the reference drug ampicillin. Compound **72c** showed less antibacterial activity against *S. aureus* with MIC values of 10.11 μm mL^{-1} and 2.53 μm mL^{-1} against *E. coli*, respectively, than ampicillin (Table 12). In addition, molecular docking studies were conducted to detect the binding modes comparable to the co-crystalized ligand ampicillin, and the designated compound **72a** displayed an extra binding mode compared to ampicillin through H-bond interaction with ARG458, DG9 and DG8 and interaction residues with DC13 and DG9. SAR analysis revealed that the introduction of electron-withdrawing groups as Cl and $-CF_3$ at position 5 gave highly potent antibacterial compounds **72a** and **72b** with a wide spectrum against both Gram-positive and Gram-negative bacteria. Their potency was nearly two folds more than that of ampicillin. However, derivatives bearing an electron-donating methyl substituent **72c** exhibited the lowest potency.[85]

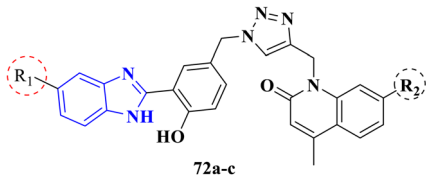

72a-c

72a: R_1= Cl, R_2= Br, (70%)
72b: R_1= CF_3, R_2= F, (74%)
72c: R_1= CH_3, R_2=F, (75%)

Fig. 15 Benzimidazole–triazole hybrids **72a–c** designed to inhibit bacterial DNA gyrase tested against *S. aureus* and *E. coli*.

Benzimidazole derivatives fused to a quinazoline moiety have been reported by Korrapati *et al.* and evaluated for their antibacterial activity (Fig. 16). The synthesized compounds were tested against three Gram-positive bacteria, *S. aureus*, *B. subtilis* and *M. luteus*, and one Gram-negative bacteria, *K. planticola*. Compounds **73a–d** displayed excellent antibacterial activity with MIC values ranging from 3.9 μg mL^{-1} to >125 μg mL^{-1} through inhibition of DNA gyrase, leading to the inhibition of replication, transcription and recombination, which resulted in the death of the microbial organism. Compound **73c** exhibited outstanding activity against *S. aureus*, *B. subtilis* and *M. luteus* with an MIC value of 3.9 μg mL^{-1} comparable to the MIC value of the reference drug ciprofloxacin 0.9 μg mL^{-1} (Table 13). The good activity of compounds **73a** and **73b** attributed to substitution with a fluorine atom generally against tested bacterial strains, particularly *S. aureus*, while replacing the fluorine atom with the nitro group, led to improvement in the antibacterial activity, particularly against *S. aureus*, *B. subtilis* and *M. luteus*. Furthermore, molecular docking studies of the designated compound **73c** displayed binding interactions similar to the co-crystalized ligand ciprofloxacin with amino acid residues Ile90 and Asn46. Overall, the synthesized derivatives exhibited better selectivity against Gram-positive bacteria than Gram-negative bacteria, electron-donating group substitution, methoxy substitution in compound **73d**, diminished the activity.[86]

2.1.1 Antifungal activity. Ashok and his team synthesized novel benzimidazoles linked to indole and 1,2,3 triazole moieties *via* a microwave-assisted click reaction. Compounds **74a–d**

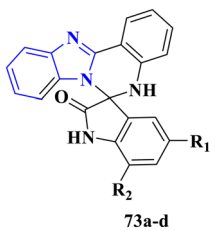

73a-d

73a: R1= F, R2= H, (92%)
73b: R1= H, R2= F, (95%)
73c: R1= NO_2, R2= H, (94%)
73d: R1= OCH_3, R2= H, (97%)

Fig. 16 Benzimidazole–quinazoline hybrids **73a–d** targeting DNA gyrase for antibacterial activity.

Table 12 MIC values of compounds **72a–c** against *S. aureus* and *E. coli*, compared to ampicillin

	Minimum inhibition concentration (μg mL^{-1})	
Compound	*S. aureus*	*E. coli*
72a	0.07	0.14
72b	0.14	0.14
72c	10.11	2.53
Ampicillin	0.27	0.26

Table 13 MIC values of compounds **73a–d** against Gram-positive and Gram-negative bacterial strains

	Minimum inhibition concentration (μg mL^{-1})			
Compound	*S. aureus*	*B. subtilis*	*M. luteus*	*k. planticola*
73a	7.8	7.8	7.8	>125
73b	7.8	7.8	7.8	>125
73c	7.8	3.9	3.9	>125
73d	>125	>125	>125	>125
Ciprofloxacin	0.9	0.9	0.9	0.9

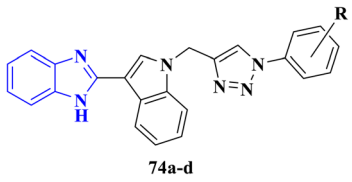

Fig. 17 Benzimidazole–triazole derivatives **74a–d** designed for antifungal evaluation against *C. albicans*.

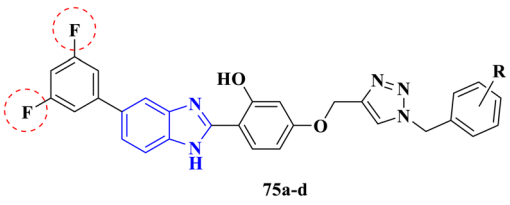

Fig. 18 Benzimidazole–triazole conjugates **75a–d** optimized for antifungal activity.

were designed and tested for their potential antifungal activity against *Candida albicans* (Fig. 17). Compounds **74a** and **74c** showed excellent antifungal activity with an equal MIC value of 6.25 μg mL^{-1} comparable to the MIC value of 1.56 μg mL^{-1} of the reference drug fluconazole by inhibiting ergosterol synthesis, a vital component of fungal cell membranes, while compound **74d** exhibited weak antifungal activity with an MIC value of 100 μg mL^{-1} (Table 14). In addition, physicochemical parameters such as the drug score were calculated, and the results showed that the designed compounds **74a** and **74c** displayed favorable drug score values. The structure–activity relationship indicated that substitution with electron-withdrawing groups either at position 2 or at position 4 had equal positive effects on the antifungal activity; however, introducing substitutions with other electron-donating groups as the methoxy group decreases the antifungal activity.[87]

In 2023, Mallikanti *et al.* reported that incorporation of benzimidazole and triazole pharmacophores significantly improved antifungal efficacy. The planar structure of these compounds **75a–d** likely facilitates the π–π stacking and T-shaped interactions within the cavity of target receptors. Compounds **75a–d** were screened against two fungal strains *C. albicans* and *A. niger* (Fig. 18). Compounds **75a** and **75b** showed excellent equipotency antifungal activities through interfering with fungal cell division with an inhibition zone diameter value of 24 μg mL^{-1}, whereas compound **75c** displayed a high inhibition zone diameter of 23 μg mL^{-1} comparable to the inhibition zone value of 18 μg mL^{-1} of the reference drug griseofulvin against *C. albicans*, while they revealed outstanding activity against *A. niger* with inhibition zone diameters of 23, 24 and 25 μg mL^{-1}, respectively in comparison to griseofulvin drug. However, compound **75d** presented an inhibition zone diameter of 9 μg mL^{-1} against *C. albicans* and 10 μg mL^{-1} against *A. niger* comparable to the control drug griseofulvin (Table 15). Moreover, molecular docking studies were conducted against secreted aspartic proteinase (Sap)1 specifically as it plays a crucial role in superficial candida infections. The designated compound **75c** presented extra binding interactions as the co-crystalized ligand griseofulvin with H-bond interactions with Asp32, Asp86, Ser88, Thr222, and Tyr225 and hydrophobic interactions with Val12, Ile30, Tyr84, Gly85, Ser88, Ile119, Ala303, and Ile305 of Sap. The results clearly indicated that introduction of electron withdrawing groups such as CN and F at positions 3 and 4 on the phenyl ring increase antifungal activity while substitution with electron donating groups as methyl reducing antifungal activity. Moreover 2,4 difluro-moiety at position 5 optimal for activity.[88]

Table 14 MIC values of compounds **74a–d** against *C. albicans*

Compound	Minimum inhibition concentration (μg mL^{-1})
	C. albicans
74a	6.25
74b	6.25
74c	6.25
74d	100
Fluconazole	1.56

Table 15 Inhibition zone diameters of compounds **75a–d** against *C. albicans* and *A. niger*

Compound	Diameter inhibition zone (μg mL^{-1})	
	C. albicans	*A. niger*
75a	24	23
75b	24	24
75c	23	25
77d	9	10
Griseofulvin	18	18

Benzimidazole derivatives containing 1,2,4 triazole moieties were synthesized by Kankite and his team to obtain hybrids **76a–c** (Fig. 19). Compounds were tested against one fungal strain *C. albicans in vitro* with an additional benefit of *in vivo* screening by the kidney burden test. Compound **76a** exhibited excellent antifungal activity at a concentration of 0.0075 μM mL^{-1} (Table 16), which is equipotent to fluconazole activity by inhibiting ergosterol biosynthesis through binding to 14-α-demethylase (CYP51) causes membrane dysfunction resulted in death of the fungi. While compounds **76b** and **76c** showed less antifungal activity at equal values, 0.015 μM mL^{-1}. Furthermore, a molecular modeling study was conducted to detect appropriate binding

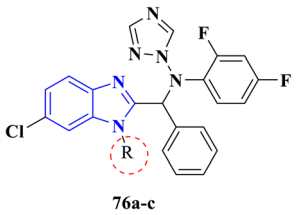

Fig. 19 Benzimidazole–triazole hybrids **76a–c** acting on CYP51 for antifungal activity.

Table 16 MIC values of compounds **76a–c** against *C. albicans*

Compound	Minimum inhibition concentration (μM mL^{-1}) *C. albicans*
76a	0.0075
76b	0.015
76c	0.015
Fluconazole	0.0075

with the targeted enzyme CYP51, the designated compound **76a** is positioned perpendicular to the porphyrin plane, and a heme iron is highly coordinated with a ring nitrogen N4 as the co-crystalized ligand fluconazole, presenting the same binding. The structure–activity relationship illustrated that the antifungal activity increased through the introduction of phenyl ring at position 1, while the antifungal activity reduced with the increase in the alkyl length of N1 of the benzimidazole nucleus (methyl to ethyl). Compounds displayed high safety margin supported by kidney burden test so inducing highly safe antifungal candidates.[89]

In the *in vitro* studies by Evren *et al.*, new benzimidazole derivatives including triazole moieties were synthesized to evaluate their activity. Compounds **77a–c** were screened for antifungal activity against *C. albicans* fungal strains (Fig. 20). Compounds **77a** exhibited outstanding activity against the fungal strain with an MIC value of 3.9 μg mL^{-1} rather than the MIC value of the reference drug ketoconazole 7.8 μg mL^{-1} acting by the inhibition of ergosterol biosynthesis, which resulted in fungicidal action while compound **77b** showed equipotent MIC as the control drug ketoconazole. However, compound **77c** implied weak antifungal activity with an MIC value >1 mg mL^{-1} (Table 17). Furthermore, molecular docking analysis against 14-α-demethylase (CYP51) revealed that the designated compound **77a** displayed similar binding modes as the co-crystalized ligand through pi–pi stacking interactions with Hie377. Moreover, extra binding modes with hydrogen bond interactions with Met508 and hydrophobic interactions with Leu376 and Tyr64 are observed. In addition, ADMET studies were performed for the synthesized compounds and

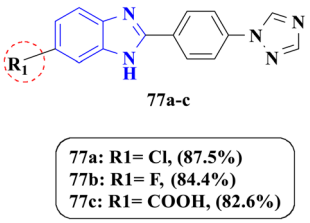

Fig. 20 Benzimidazole–triazole compounds **77a–c** evaluated for antifungal potency against *C. albicans*.

Table 17 MIC values of compounds **77a–c** against *C. albicans*

Compound	Minimum inhibition concentration (μg mL^{-1}) *C. albicans*
77a	3.9
77b	7.8
77c	>1 mg mL^{-1}
Ketoconazole	7.8

presented compounds have good oral bioavailability with high safety margin. Evidently, direct attachment between triazole and phenyl rings resulting in compounds with planar conformation as compounds **77a** and **77b** increased the antifungal potency.[90]

In recent investigations by Ghobadi *et al.*, a series of benzimidazole-bearing triazole moieties were designed as a hybrid of mebendazole **78a–c** against two fungal strains *C. albicans* and *C. neoformans* (Fig. 21). Compounds **78a** and **78b** exhibited excellent antifungal activity against *C. albicans* with an equipotent MIC value <0.063 μg mL^{-1}, their MIC values were 2- to 8-fold higher than that of the reference drug fluconazole (0.5 μg mL^{-1}). Compound **78a** also showed good antifungal activity against *C. neoformans* with an MIC value of 1 μg mL^{-1} and compound **78b** exhibited outstanding activity against *C. neoformans* with an MIC value of 0.125 μg mL^{-1}, when compared to the MIC value of the reference drug fluconazole 0.5 μg mL^{-1}. However, compound **78c** displayed weak antifungal activity against both fungal strains with MIC values of 4 μg mL^{-1} and 16 μg mL^{-1}, respectively, comparable to the

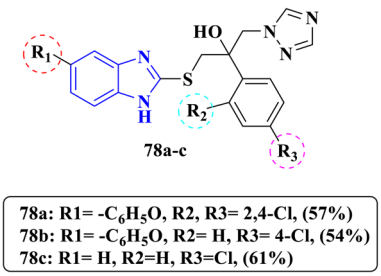

Fig. 21 Benzimidazole–triazole analogs **78a–c** screened against *Candida* and *Cryptococcus* species.

Table 18 MIC values of compounds **78a–c** against *C. albicans* and *C. neoformans*

Compound	Minimum inhibition concentration (μg mL^{-1})	
	C. albicans	*C. neoformans*
78a	<0.063	1
78b	<0.063	0.125
78c	4	16
Fluconazole	0.5	0.5

MIC value of the reference drug fluconazole (Table 18). According to SAR analysis, substitution at position 5 in the benzimidazole with a bulky benzoyl group positively affected the antifungal activity. However, a simplification strategy by removing a benzoyl moiety gave weak antifungal agents, while variation in halogens substituents in the phenyl ring gave equipotent compounds, but it mainly depends on the type of the side chain. Docking studies as mentioned displayed high binding in the active site of lanosterol 14α-demethylase (CYP51) through a coordination bond between the N4 in the triazole ring and heme iron with a distance 2.7 Å as well as, the designated synthesized compounds**78a** and **78b** displayed desirable ADMET properties and drug-likeness more than the reference drug fluconazole. In addition, they showed high profile safety margin with no carcinogenic probability.[91]

A novel series of benzimidazole hybridized with 1,2,4 triazole moiety was designed by Güzel and colleagues, compounds were investigated to evaluate their antifungal activity against four fungal strains of *Candida*, *C. albicans*, *C. glabrata*, *C. krusei* and *C. parapsilopsis* (Fig. 22). Compounds **79a–d** exhibited outstanding activity against only one fungal strain *C. glabrata*, compounds **79b–79c** showed an equipotent MIC value of 0.97 μg mL^{-1} greater than the MIC value of 1.95 μg mL^{-1} of the reference drug voriconazole, while compound **79d** displayed antifungal activity with an MIC value equal to that of the control drug voriconazole (Table 19). Furthermore, a molecular docking study was conducted on the most active compounds **79b–79c** and displayed binding interactions similar to voriconazole with Tyr118, His377 and Hem601 residues, and the interactions with HEM present in 14 α demethylase (CYP51) were seen as π–π stacking and π-cation interactions, presenting high antifungal activity found in the designated compounds. In addition, Scanning Electron Microscopy with Energy-Dispersive X-ray analysis (SEM-EDX) was used to observe the surface morphology of *C. glabrata* before and after the test compound treatment, the SEM results displayed cell wall deformations and loss of membrane integrity as the reference drug voriconazole. The SAR analysis proved that all compounds substituted at position 4 either with bulky groups as a methoxy group or with large radius groups as a chlorine atom fruitfully affect the antifungal activity. Moreover, the phenyl ring was substituted with different groups; from the screening results, we can conclude that potent compounds **79a–79c** bear chloro and

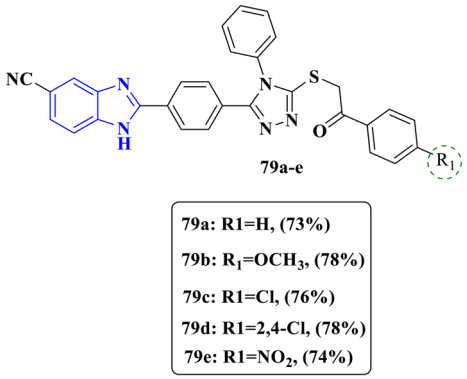

Fig. 22 Benzimidazole–triazole hybrids **79a–e** evaluated for anti-candidal activity.

Table 19 MIC values of compounds **79a–e** against *C. glabrata*

Compound	Minimum inhibition concentration (μg mL^{-1})
	C. glabrata
79a	1.95
79b	0.97
79c	0.97
79d	1.95
79e	1.95
Voriconazole	1.95

methoxy groups. Substitution mainly in the phenyl ring at position C-4 was crucial for the anticandidal activity.[92]

The work by Aaghaz and his team reported novel benzimidazole scaffolds bearing thiazole and morphiline moieties inducing significant antifungal activities, and compounds **80a–c** were investigated against three fungal strains *C. neoformans*, *C. albicans* and *C. parapsilosis* (Fig. 23). Compound **80a** displayed little antifungal activity against the tested fungal strains with an equivalent MIC value of 81.6 μg mL^{-1} comparable to the MIC value of the control drug amphotericin 1 μg mL^{-1}, while compound **80b** exhibited excellent antifungal activity against the mentioned strains with MIC values of 2.4 μg mL^{-1}, 4.9 μg mL^{-1} and 19.6 μg mL^{-1}, respectively, comparable to amphotericin drug. Moreover, compound **80c** exhibited good activity against both *C. neoformans* and *C. albicans* with MIC values of 9.7 μg mL^{-1} and 38.7 μg mL^{-1}, respectively, and minor antifungal activities against C. *parapsilosis* with an MIC value of 155.9 μg mL^{-1} with respect to the MIC value of amphotericin (Table 20). Moreover, propidium iodide (PI) uptake study by confocal laser scanning microscopy test was utilized to detect permeability to cell membrane through a red fluorescent dye found in PI, and a promising result was observed regarding compound **80b** followed by staining with PI, leading to the permeabilization of this compound inside the fungal cells, and this has been confirmed by the presence of red fluorescence in the treated cells. In addition, the Time Kill Assay test was performed to detect time

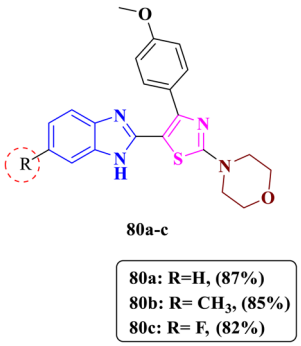

Fig. 23 Benzimidazole–thiazole–morpholine hybrids **80a–c** with promising antifungal profiles.

Table 20 MIC values of compounds **80a–c** against three *Candida* species

	Minimum inhibition concentration (μg mL^{-1})		
Compound	*C. neoformans*	*C. albicans*	*C. parapsilosis*
80a	81.6	81.6	81.6
80b	2.4	4.9	19.6
80c	9.7	38.7	155.9
Amphotericin B	1	1	1

intervals required to completely inhibit the growth of fungal cells, and it was observed that compound **80b** significantly kills *C. neoformans* after 8 h when compared to amphotericin B that inhibits the growth of *Cryptococcal* cells after 4 h, presenting an advantage of sustained activity over time. Moreover, the designated compounds displayed direct coordination with nitrogen of the azole ring to the HEM ferric ion in CYP51 belonging to cytochrome P450 that is required for the biosynthesis of ergosterol in fungi. On top of that, *in vitro* mammalian cell cytotoxicity of **80b** was performed against the human cancer cell line (HeLa) as well as normal human cell line (HEK-293) at different concentrations. The designated compound **80b** did not exhibit any significant toxicity. SAR studies demonstrated that thiazole and morpholine moieties are optimal for activity. Furthermore, substitution with a methoxy group at the *para* position diminished antifungal activity towards all fungi strains, while substitution at the *meta* position enhanced antifungal activity against all fungal strains, and introducing an electron-donating group as the methyl group at position 6 in the benzimidazole core offered promising antifungal activities particularly against *C. neoformans* and *C. albicans* **80b**; however, substitution with an electron-withdrawing group as the fluorine atom produced significant antifungal activities only towards *C. neoformans*.[93]

Through molecular hybridization, Cevik and collaborators synthesized bioactive derivatives **81a–c** in a single molecule as benzimidazole hybrids with oxadiazole moieties, providing anticandida properties through the inhibition of 14α-demethylase (Fig. 24). Compounds were screened against different species of *candida* fungal strains *C. albicans*, *C. glabrata* and *C. kruesi* using ketoconazole as the reference drug. Compound **81a** reported an excellent MIC value of 0.78 μg mL^{-1} against *C. albicans* and good antifungal activity with an MIC value of 3.12 μg mL^{-1} against both *C. glabrata* and *C. kruesi*, when compared to the MIC value of the reference drug ketoconazole 1.56 μg mL^{-1}. Compound **81b** displayed excellent antifungal activity against *C. albicans* with an MIC value of 0.78 μg mL^{-1}, mild antifungal activity against *C. glabrata* with an MIC value of 3.12 μg mL^{-1} and outstanding antifungal activity against *C. kruesi* with an MIC value of 1.56 μg mL^{-1} comparable to the ketoconazole drug. Compound **81c** exhibited significant antifungal activity against the tested fungal strains with MIC values of 1.56 μg mL^{-1} for both *C. albicans* and *C. glabrata* and 0.78 μg mL^{-1} against *C. kruesi* with respect to the reference drug ketoconazole 1.56 μg mL^{-1} (Table 21). The results were supported with molecular docking studies, displaying binding modes directly with an HEM ferrous ion in the active site of CYP51 as ketoconazole. Furthermore, molecular dynamics were performed at 100 ns simulations, and the designated compounds displayed high stability with low RMSD aligned with strong binding to the HEM. Compound **81b** showed the most stable binding followed by **81c** and **81a**. On top of that, all tested compounds showed high therapeutic safety margin by these studies and the targeted compounds offer further support to the biological results. Structure–activity relationship showed that either the absence of substitution or the introduction of an electron-withdrawing chlorine atom at position 5 enhanced antifungal activity against *Candida albicans*, as observed in compounds **81a** and **81b**, while substitution with electron donating group as methyl group showed equipotent activity to the reference drug ketoconazole **81c** against both fungi strains *C. albicans*, *C. glabrata*. They also displayed outstanding potent antifungal activity against *C. kruesi* compared with ketoconazole.[94]

In their 2023 study, Pham *et al.* designed and synthesized novel benzimidazole scaffolds **82a–82c** *via* the alkylation of N1 of benzimidazole inducing antifungal activity (Fig. 25). Compounds were screened against two fungal strains of *C. albicans* and *A. niger*. Compound **82b** displayed excellent antifungal activity with MIC values of 16 μg mL^{-1} against *C. albicans* when compared to the reference drug fluconazole 4 μg mL^{-1} and outstanding activity against *A. niger* with an MIC value of 32 μg mL^{-1} compared to the MIC of the fluconazole drug 128 μg mL^{-1}. Compound **82a** showed less antifungal activity against both fungal strains with an equal MIC value of 512 μg mL^{-1}

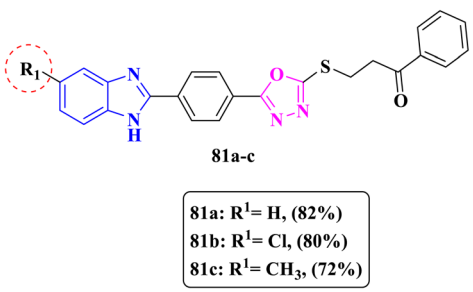

Fig. 24 Benzimidazole–oxadiazole conjugates **81a–c** targeting *Candida* species.

Table 21 MIC values of compounds **81a–c** against *C. albicans*, *C. glabrata*, and *C. krusei*

Compound	Minimum inhibition concentration (μg mL^{-1})		
	C. albicans	*C. glabrata*	*C. krusei*
81a	0.78	3.12	3.12
81b	0.78	3.12	1.56
81c	1.56	1.56	0.78
Ketoconazole	1.56	1.56	1.56

Table 22 MIC values of compounds **82a–c** against *C. albicans* and *A. niger*

Compound	Minimum inhibition concentration (μg mL^{-1})	
	C. albicans	*A. niger*
82a	512	512
82b	16	32
82c	128	128
Fluconazole	128	128

against *C. albicans* and *A. niger* with respect to the fluconazole drug. Moreover, compound **82c** exhibited minor antifungal activity against *C. albicans* with an MIC value of 128 μg mL^{-1} looking at the MIC value of fluconazole drug and good antifungal activity against *A. niger* with equipotent MIC value of fluconazole drug 128 μg mL^{-1} compared to fluconazole (Table 22). Moreover, molecular docking studies revealed that compound **82b** established one strong hydrogen bond with Tyr225 resembling the co-crystallized ligand fluconazole with *N*-myristoyltransferase (NMT), which is crucial for fungal viability. Moreover, it is involved in key processes such as cell wall synthesis, morphogenesis, and signal transduction. Additionally, compound **82b** exhibited an excellent ADMET profile with a high safety margin, and hence, it is recommended to be a lead-like compound for further drug development. SAR analysis revealed that the benzyl moiety was optimal for activity when replaced with an allyl moiety, where the antifungal activity was reduced in **82a**. Moreover, substitution on the phenyl ring at position 4 with large radius groups such as chlorine, as in compound **82b**, was associated with enhanced antifungal activity.in compound **82b**, was associated with enhanced antifungal activity. Moreover, the introduction of one more chlorine atom at position 3 diminished activity as in derivative **82c**.[95]

Morcoss and collaborators designed novel benzimidazole scaffolds incorporated with hydrazone moieties **83a–e** and then investigated their antimicrobial activity against two fungal strains *C. albicans* and *C. neoformans* (Fig. 26). Compounds **83a–e** exhibited significant antifungal activity against *C. albicans* and *C. neoformans* with MIC values ranging from 4 μg mL^{-1} to >32 μg mL^{-1}, comparable to the reference drug fluconazole with values 0.125 μg mL^{-1} and 8 μg mL^{-1}, respectively. Compound **83a** showed excellent activity comparable to other compounds with MIC values of 4 μg mL^{-1} and 16 μg mL^{-1} against the two

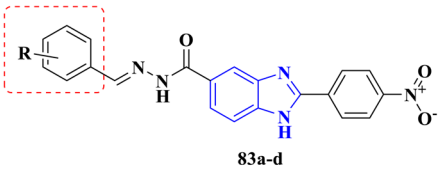

83a:R= H, (80%)
83b:R= F, (60%)
83c:R=4-Cl, (83%)
83d:R=2,4-Cl, (73%)
83e:R=3,4,5-tri-OCH$_3$, (81%)

Fig. 26 Benzimidazole–hydrazone derivatives **83a–e** with antifungal efficacy.

fungal strain, respectively, comparable to the MIC value of the control drug fluconazole. Compound **83c** revealed good antifungal activity against *C. albicans* and *C. neoformans* with an MIC value of 16 μg mL^{-1} when compared to the reference drug fluconazole, while compound **83d** displayed good activity against *C. albicans* with an MIC value of 8 μg mL^{-1} and an MIC value >32 μg mL^{-1} against *C. neoformans*. However, both compounds **83b** and **83e** displayed MIC more than 32 μg mL^{-1} with less antifungal activity (Table 23). Additionally, Sterol Quantitation Method (SQM) used a spectrophotometric assay to measure the effect of antifungal drugs that inhibit sterol biosynthesis, and compound **83a** efficiently inhibited the ergosterol biosynthesis in the fungal cell membrane by binding to sterol 14α-demethylase like the reference drug ketoconazole. Furthermore, the designated compound **83a** exhibited high safety margin against red blood cells and human embryonic kidney cells at a concentration up to 32 μg mL^{-1}. Moreover, compound **83a** exhibited excellent pharmacokinetic properties,

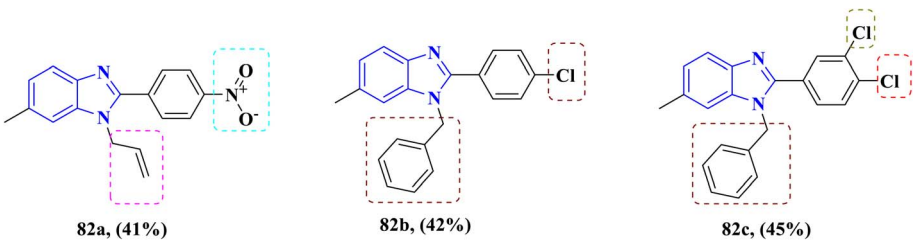

82a, (41%) **82b, (42%)** **82c, (45%)**

Fig. 25 N1-substituted benzimidazoles **82a–c** screened for antifungal activity.

Table 23 MIC values of compounds **83a–e** against *C. albicans* and *C. neoformans*

Compound	Minimum inhibition concentration (μg mL^{-1})	
	C. albicans	*C. neoformans*
83a	4	16
83b	>32	>32
83c	16	16
83d	8	>32
83e	>32	>32
Fluconazole	0.125	0.125

characterized by high oral bioavailability. The results were supported with molecular docking studies and revealed that compound **83a** showed binding modes interaction with HEM as the co-crystallized ligand fluconazole. SAR analysis could be interpreted that an unsubstituted phenyl ring and the introduction of a chlorine atom at position 4 increased the activity against both *C. albicans* and *C. neoformans* while substitution with chlorine atom at positions 2,4 increased antifungal activity against only *C. albicans*; however, substitution with either electron-donating groups or small halogen groups as fluorine atoms abolished antifungal activity.[96]

In 2021, Chaurasi and his team designed and synthesized benzimidazole nucleoside analogues containing a glycoside linkage, as variable chemical scaffolds yielded targeted derivatives **84a–84c** (Fig. 27), and compounds were investigated against four fungal strains *C. albicans*, *A. niger*, *Aspergillus flavus* and *Fusarium oxysporum*. Notably synergistic effects of these moieties offered excellent activity against three fungal strains *C. albicans*, *A. flavus* and *F. oxysporum*. Compounds **84a** and **84c** exhibited significant antifungal activity against *C. albicans*, *A. flavus* and *F. oxysporum*, with MIC values ranging from 0.78 μg mL^{-1} to 12.5 μg mL^{-1} compared with the MIC values of 3.12, 1.56 and 12.5 μg mL^{-1} of the reference drug ketoconazole, respectively. Furthermore, compound **84b** showed lesser antifungal activity against tested strains, with MIC values of 50, 25 and 100 μg mL^{-1} respectively, than the control drug ketoconazole (Table 24). Density functional theory (DFT) calculations

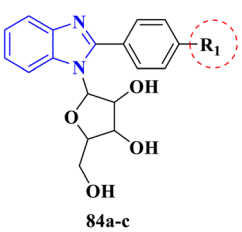

Fig. 27 Benzimidazole–isoxazole hybrids **84a–c** against fungal strains.

Table 24 MIC values of compounds **84a–c** against fungal strains

Compound	Minimum inhibition concentration (μg mL^{-1})		
	C. albicans	*A. flavus*	*F. oxysporum*
84a	1.56	1.56	6.25
84b	50	25	100
84c	3.12	0.78	12.5
Ketoconazole	3.12	1.56	12.5

were performed to study the electronic properties of compounds **84a** and **84c** and to support the biological results, and demonstrated that compounds with lower HOMO–LUMO energy gaps, particularly compound **84a**, exhibited excellent antifungal activity against *C. albicans* as fluconazole. The reduced bandgap energy (ΔE) facilitated efficient intramolecular charge transfer and stronger interactions with fungal biomolecules. SAR analysis proved that position 4 in the phenyl ring is important for antifungal activity and it must be free of substitutions for the most potent antifungal agent **84a** or incorporated with hydrophilic group as OH group **84c**; however, increasing lipophilicity through substitution with electron-withdrawing groups as bromine diminished the activity **84b**. Moreover, *in silico* ADMET study supported that the compounds could be developed to be good antifungal candidates.[97]

2.1.2 Dual (antibacterial and antifungal) activities. A novel series of benzimidazole scaffolds bearing quinolone hybrids **85a–85d**, **86a–86b** and **87a–87e** were synthesized and investigated by Wang *et al.* for their antimicrobial activities (Fig. 28). All compounds were screened against three strains of Gram-positive bacteria (*MRSA*, *E. faecalis* and *S. aureus*), four strains of Gram-negative bacteria (*K. pneumoniae*, *E. coli*, *P. aeruginosa* and *A. baumanii*) and four fungal strains (*C. albicans*, *C. tropicalis*, *A. fumigatus* and *C. parapsilosis*). Compounds **85a–85d** exhibited excellent antibacterial activity against *MRSA* with MIC values ranging from 8 μg mL^{-1} to 128 μg mL^{-1} compared to the reference drugs norfloxacin and clinafloxacin with MIC values >512 μg mL^{-1} and significant activity against *K. pneumoniae* with MIC values ranging from 8 μg mL^{-1} to 256 μg mL^{-1} compared to the reference drugs norfloxacin and clinafloxacin with MIC values 32 μg mL^{-1} and >512 μg mL^{-1}, respectively, while compounds **86a–86b** displayed good activity against *MRSA* with MIC values 8 μg mL^{-1} and 128 μg mL^{-1} and gentle activity against *P. aeruginosa* with equal MIC values 32 μg mL^{-1} comparable to the MIC values of the reference drugs of 32 μg mL^{-1} and 4 μg mL^{-1} respectively. Furthermore, series of compounds **87a–87e** showed the most outstanding activity against both MRSA with MIC values ranging from 8 μg mL^{-1} to 256 μg mL^{-1} and *P. aeruginosa* with MIC values ranging from 1 μg mL^{-1} to 16 μg mL^{-1}, particularly compound **87b** presented excellent antibacterial activity against *P. aeruginosa* with an MIC value of 1 μg mL^{-1}, for which the potency was 4- and 32-fold greater than that of the reference drugs norfloxacin and clinafloxacin (Table 25). Furthermore, molecular docking study revealed that compound **87b** has strong inhibitory activity to

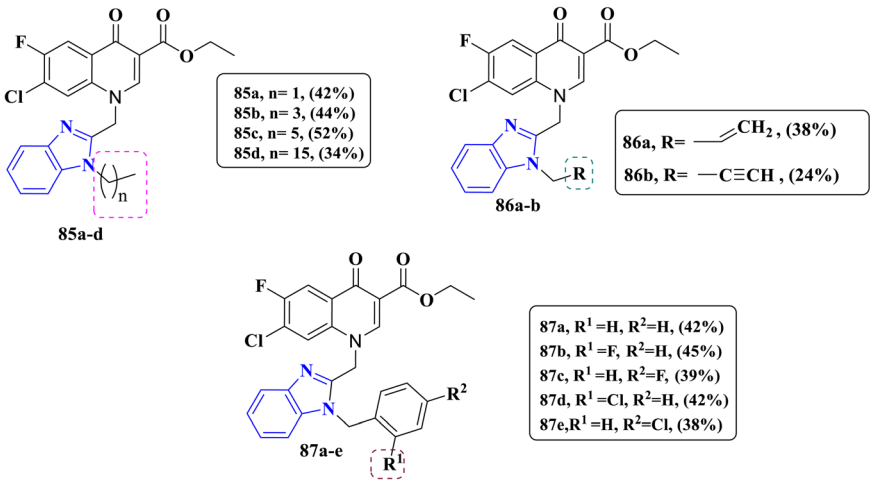

Fig. 28 Benzimidazole derivatives **85a–d**, **86a–b** and **87a–e** designed for dual antimicrobial activity.

Table 25 MIC values of compounds **85a–d**, **86a–b** and **87a–e** against bacterial and fungal strains

	Minimum inhibition concentration (μg mL^{-1})			
Compound	*MRSA*	*K. pneumoniae*	*P. aeruginosa*	*C. tropicalis*
85a	16	8	64	16
85b	8	8	512	16
85c	16	8	256	128
85d	128	256	256	256
86a	8	64	32	128
86b	128	128	32	512
87a	64	4	4	4
87b	8	16	1	1
87c	128	4	16	64
87d	64	64	8	256
87e	256	256	32	256
Norfloxacin	>512	32	32	—
Clinafloxacin	>512	>512	4	—
Fluconazole	—	—	—	256

topoisomerase IV altering DNA topology by generating a double-stranded break in the genetic material presenting similar binding modes to the Gly419 residue and base D16 of DNA through hydrogen bonding at distances of 2.4 and 2.1 A° with the co-crystallized ligand moxifloxacin. Moreover, the designated compound **87b** displayed excellent binding modes as the co-crystallized ligand with fluconazole with HEM. Additionally, the derivative **87b** displayed high safety profile against human laryngeal carcinoma epithelial cells. The SAR insights for compounds **85a–d** revealed that the length of the aliphatic chain bearing in the benzimidazole nucleus affected by length of aliphatic chain, since short ethyl chain demonstrated greater efficacy as antibacterial agents than those with hexadecyl chain. In addition, it was shown that the unsaturated aliphatic chains have a less inhibitory effect, thus presenting poor antibacterial activity in compounds **86a–b**, and the presence of a fluorine atom increases the antibacterial activity and inducing a wide spectrum against Gram-positive and Gram-negative bacteria. Mentioned compounds exhibited outstanding antifungal activity against *C. tropicalis* with MIC values ranging from 1 μg mL^{-1} to 256 μg mL^{-1} with respect to the MIC value of the reference drug fluconazole 256 μg mL^{-1}. Specifically, compound **87b** showed better antifungal activity with 256-fold more than the control drug fluconazole. In addition, alkyl-unsaturated allyl substituted compounds **85a–85d** and **86a–b** had moderate antifungal activity. Moreover, it became clear that fluorobenzyl compounds **87b–c** exhibited similar or even more potent antifungal properties compared with chlorobenzyl compounds **87d–e**. This suggests that the presence of a fluorine atom on the phenyl groups had a positive effect on inhibiting microbial growth.[98]

The research by Yadv and colleagues designed novel benzimidazole derivatives **88a–88f** incorporated with benzoyl and different substituted acetamides for inducing the antimicrobial activity (Fig. 29). The synthesized compounds were investigated for their activities against five bacterial strains (*S. aureus*, *B. cereus*, *B. subtilis*, *S. typhi* and *E. coli*), and two fungal strains (*C. albicans* and *A. niger*). Compounds **88a–d** displayed excellent antibacterial activity against *S. aureus* with an equipotency MIC value of 0.027 μM mL^{-1} comparable to the MIC value of the reference drug cefadroxil of 0.37 μM mL^{-1}, while compounds **88e–f** had good antibacterial activity with MIC values 0.031 μM mL^{-1} and 0.030 μM mL^{-1}. Furthermore, compounds **88a–d** exhibited significance antifungal activity against *A. niger*, with an equipotency MIC value of 0.027 μM mL^{-1} comparable to the MIC value of the reference drug fluconazole 0.47 μM mL^{-1}, while compounds **88e–f** showed good antifungal activity with MIC values 0.031 μM mL^{-1} and 0.030 μM mL^{-1} when compared to the control drug fluconazole (Table 26). From the obtained results, we can conclude that the antimicrobial activity were not positively affected by substitutions on the phenyl ring, either with electron-withdrawing groups as Cl, Br and NO_2 or with electron-donating group as CH_3 and OCH_3 against all bacterial and fungal tested strains.[99]

Carvacrol is a phenolic monoterpene derivative produced naturally, where hybrid compounds for medical use were

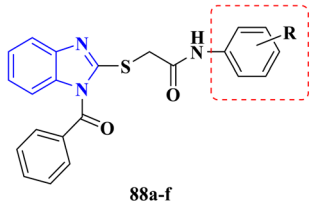

88a-f

88a: R= 2-Br, (76%)
88b: R= 3-Br, (83%)
88c: R= 4-Br, (72%)
88d: R= 3-NO_2, (78%)
88e: R= 4-CH_3, (81%)
88f: R= 4-OCH_3, (79%)

Fig. 29 Benzimidazole derivatives **88a–f** evaluated for dual antimicrobial activity.

Table 26 MIC values of compounds **88a–f** against *S. aureus* and *A. niger*

	Minimum inhibition concentration (μM mL^{-1})	
Compound	*S. aureus*	*A. niger*
88a	0.027	0.027
88b	0.027	0.027
88c	0.027	0.027
88d	0.027	0.027
88e	0.031	0.031
88f	0.030	0.030
Cefadroxil	0.037	—
Fluconazole	—	0.047

developed. Bhoi *et al.* designed benzimidazole derivatives **89a–f** developed from 2-formyl carvacrol screened and evaluated against one Gram-positive bacteria *S. aureus* and two Gram-negative bacteria *P. aeruginosa*, *E. coli*, and two fungal strains (*C. albicans* and *A. niger*) (Fig. 30). Compounds **89a–d** showed exceptional activity against *S. aureus* with MIC values ranging from 12.5 μg mL^{-1} to 250 μg mL^{-1} comparable to the MIC value of the reference drug ciprofloxacin 50 μg mL^{-1} and excellent activity against *P. aeruginosa* and *E. coli* with MIC values ranging from 12.5 μg mL^{-1} to 250 μg mL^{-1} when compared to the MIC value of the control drug chloramphenicol 50 μg mL^{-1}. Compound **89b** displayed outstanding antibacterial activity against *E. coli* while compound **89c** displayed the lowest MIC value leading to greater antibacterial activity against *S. aureus* strains. Compounds **89e–f** displayed equipotence activity against *C. albicans* with an MIC value of 250 μg mL^{-1} comparable to the reference drug griseofulvin with an MIC value of 500 μg mL^{-1} (Table 27). The ADME predictions displayed that compounds **89e** and **89f** have reliable pharmacokinetic properties. Structure–activity relationship can be illustrated by increasing the antibacterial activity either through bioisosteric replacement by introduction pyridine moiety instead of phenyl ring towards Gram-positive bacteria **89c** or by introducing electron-donating group as the methyl group increases the

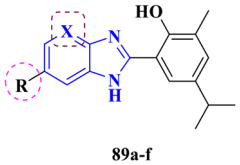

89a-f

89a: R= H, X=CH, (85%)
89b: R= CH_3, X= CH, (83%)
89c:R= H, X= N, (82%)
89d: R= CF_3, X= CH, (82%)
89e: R= F, X= CH, (89%)
89f:R= Br, X= CH, (87%)

Fig. 30 Carvacrol-derived benzimidazole hybrids **89a–f** screened for antibacterial and antifungal activity.

activity against Gram-negative bacteria **89b**; however, substitution at position 6 with halogens increases antifungal activity against *C. albicans* **89e–f**.[100]

Recently, Liu and his team designed novel benzimidazole derivatives inducing the antimicrobial activity, where they were incorporated with chalcone **90a–c**, *N*-alkyl benzimidazolyl chalcones **91a–c** and pyrimidines moieties **92a–c** and **93a–99c** (Fig. 31). The compounds were investigated against four Gram-positive bacteria (*Staphylococcus aureus*, *Methicillin-Resistant Staphylococcus aureus*, *Bacillus subtilis* and *Micrococcus luteus*) and six Gram-negative bacteria (*Bacillus proteus*, *Escherichia coli*, *Pseudomonas aeruginosa*, *Bacillus typhi*, *Escherichia coli* and *Shigella dysenteriae*) and five fungi (*Candida albicans* and *Candida mycoderma*, *Candida utilis*, *Saccharomyces cerevisiae* and *Aspergillus flavus*). Compounds **90a–c** displayed good antibacterial activity against *B. subtilis* and *B. proteus* with MIC values ranging from 4 μg mL^{-1} to 512 μg mL^{-1} comparable to the MIC value of the reference drug chloromycin 32 μg mL^{-1}. Compound **90a** exhibited an equipotence MIC activity value of 8 μg mL^{-1} against *B. subtilis* with chloromycin and excellent MIC activity value 4 μg mL^{-1} against *B. proteus* than the control drug chloromycin; moreover, they revealed great activity against *C. utilis* with MIC values ranging from 16 μg mL^{-1} to 512 μg mL^{-1}. Compound **90a** demonstrated an equipotence MIC value of 16 μg mL^{-1} compared to the reference drug fluconazole.

Table 27 MIC values of compounds **89a–f** against *S. aureus*, *P. aeruginosa*, *E. coli*, and *C. albicans*

	Minimum inhibition concentration (μg mL^{-1})			
Compound	*S. aureus*	*P. aeruginosa*	*E. coli*	*C. albicans*
89a	50	100	62.5	500
89b	62.5	50	12.5	500
89c	12.5	50	25	500
89d	250	250	50	500
89e	125	125	100	250
89f	500	250	100	250
Ciprofloxacin	50	—	—	—
Chloramphenicol	—	50	50	—
Griseofulvin	—	—	—	500

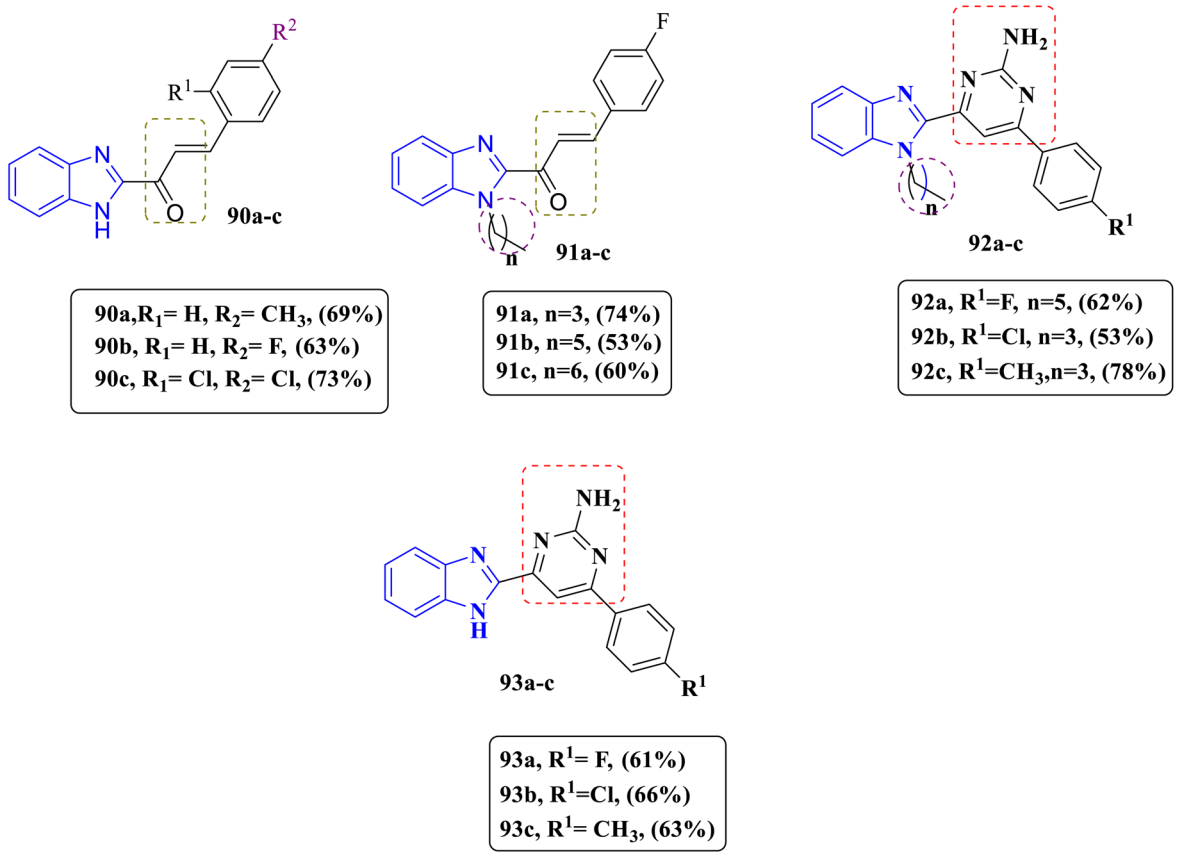

Fig. 31 Benzimidazole hybrids **90a–c**, **91a–c**, **92a–c** and **93a–c** designed for dual antimicrobial evaluation.

Compounds **91a–c** proved perfect activity against *S. aureus* and *P. aeruginosa* with MIC values ranging from 0.5 μg mL^{-1} to 512 μg mL^{-1} compared to the MIC values of the reference drug norfloxacin of 8 μg mL^{-1} and 1 μg mL^{-1}, respectively. Compound **91a** exhibited higher activity against *S. aureus* and *P. aeruginosa* than norfloxacin with MIC values of 4 μg mL^{-1} and 0.5 μg mL^{-1}. Furthermore, they expressed outstanding activity against *C. utilis* ranging from 16 μg mL^{-1} to 512 μg mL^{-1}. Compound **91a** exhibited equipotence high activity against *C. utilis* with an MIC value of 16 μg mL^{-1} comparable to the reference drug fluconazole. Compounds **92a–c** outlined excellent antibacterial activity against *S. aureus* and *P. aeruginosa* with MIC values ranging from 8 μg mL^{-1} to 512 μg mL^{-1} comparable to the MIC values of the reference drug chloromycin of 8 μg mL^{-1} and 16 μg mL^{-1}, respectively. Compound **92c** displayed outstanding antibacterial activity with an equipotence MIC value of 8 μg mL^{-1} compared to the reference drug chloromycin against *S. aureus* and great activity against *P. aeruginosa* more than the control drug chloromycin with MIC values of 8 μg mL^{-1} and 16 μg mL^{-1} against chloromycin drug. In addition, they revealed excellent antifungal activity against *C. utilis* ranging from 2 μg mL^{-1} to 8 μg mL^{-1} when compared with the MIC value of the reference drug fluconazole 16 μg mL^{-1}. Compound **92b** proved antifungal activity that is 8-fold more potent than the fluconazole drug. Compounds **93a–c** showed excellent antibacterial activity against *S. aureus* and *P. aeruginosa* with MIC values ranging from 2 μg mL^{-1} to 128 μg mL^{-1} comparable to the MIC value of the reference drug chloromycin. Compounds **93a–93c** displayed good antibacterial activity with MIC values of 2 μg mL^{-1} and 8 μg mL^{-1} against *S. aureus* comparable to the MIC value of 8 μg mL^{-1} of the reference drug chloromycin and great activity against *P. aeruginosa* with MIC values of 16 μg mL^{-1} and 4 μg mL^{-1}, respectively. In addition, they exhibited exceptional antifungal activity against *A. flavus* with an MIC value ranging from 1 μg mL^{-1} to 256 μg mL^{-1} with respect to the MIC value of the reference drug fluconazole 250 μg mL^{-1} (Table 28). Compound **90d** showed excellent activity that is 256-fold more than that of fluconazole drug. In addition, DNA binding studies were performed to detect interaction with DNA by intercalation, groove binding, or electrostatic interactions. The results indicated that the designated compound **93c** highly binds to DNA and blocks replication, explaining its antimicrobial effects. Moreover, molecular docking studies displayed that compound **93c** strongly binds to DNA gyrase, resulting in the inhibition of DNA replication *via* forming a hydrogen bond with Asp1083 through NH and NH_2 groups, and additional interactions were detected with Arg1122, Met1121, Ala1120, and Tyr1087. Furthermore, Molecular Electrostatic Potential (MEP) analysis was used to visualize how a drug or ligand would fit and bind to its target; as a result, compound **93c** showed strong positive regions around NH_2 and NH, favorable for target binding supporting of molecular

Table 28 Antimicrobial MIC data for benzimidazole derivatives **90a–c**, **91a–c**, **92a–c** and **93a–c**

	Minimum inhibition concentration (μg mL^{-1})					
Compound	*B. subtilis*	*B. proteus*	*S. aureus*	*P. aeruginosa*	*C. utilis*	*A. flavus*
90a	16	4	8	4	16	16
90b	64	32	16	128	>512	512
90c	64	512	128	512	64	512
91a	4	512	4	0.5	16	128
91b	256	64	512	512	512	16
91c	512	512	512	512	>512	512
92a	512	128	512	128	512	512
92b	64	4	16	64	256	256
92c	16	16	8	8	64	64
93a	2	128	2	16	256	256
93b	64	8	64	128	4	4
93c	8	1	8	4	1	1
Chloromycin	32	32	8	16	—	—
Norfloxacin	2	4	8	1	—	—
Fluconazole	—	—	—	—	16	256

docking study. On top of that, compound **93c** exhibited low toxicity against human hepatocyte (LO2) cells, suggesting a good safety profile. The SAR results indicated that chalcone and pyrimidine moieties are optimal for antimicrobial activity, in case of chalcone derivatives as in derivatives **90a–c** and **91a–c**, introduction of electron donating groups as methyl group increase the activity towards both bacterial and fungal strains while introducing electron withdrawing groups as chlorine or fluorine atoms resulted in minor antimicrobial activities. While alkylation of NH in the benzimidazole ring with different small and long aliphatic chains, studies revealed that propyl chain has more potent antimicrobial activity > pentyl > heptyl. However, pyrimidine derivatives **91a–c** and **92a–c** offered promising antimicrobial activities and also the chain length of alkylated NH is essential for activity as chalcone derivative substitution in the *para* position with an electron-withdrawing group as chlorine atom **92b** increased activity towards bacterial strains, while substitution with an electron-donating group as methyl group **92c** increased antifungal activity towards *C. utilis*. Additionally, NH-free benzimidazole analogs, such as in the designated compounds **93a–c**, exhibited potent antimicrobial activity, introduction of electron donating group as methyl group at position 4 increase antibacterial activity against Gram-negative bacteria *P. aeruginosa* and outstanding antifungal activity against *A, flavus*, while incorporation with electron withdrawing group as fluorine atom increase activity towards Gram-positive bacteria *S. aureus*.[101]

2.1.3 Antiviral activity. Francesconi *et al.* investigated two series of benzimidazole derivatives (thio), semicarbazones and hydrazones, synthesized from 5-acetyl benzimidazoles to evaluate their antiviral efficacy (Fig. 32). Compounds **94a** and **94b** displayed a dual inhibitory activity against *Influenza A* and *Human corona virus* as the first benzimidazole derivatives reported activity against *Corona virus*. Compound **94a** exhibited good activity against both *Influenza A* and *HCV* with $EC_{50} = 38$ μM and 56 μM, respectively, comparable to the EC_{50} of the reference drug ribavirin 7.5 μM; moreover, compound **94b** showed outstanding activity against both viruses with $EC_{50} = 25$ μM and 38 μM, respectively, when compared to the reference drug ribavirin. Compounds **94c** and **94d** exhibited potent and selective activity against respiratory syncytial virus (RSV) by inhibiting viral RNA synthesis. Their EC_{50} values were (7 μM and 2.4 μM, respectively) comparable to the reference drug ribavirin (6.7 μM) (Table 29). Molecular modelling studies for the designated compounds **94c** and **94d** properly bind to the exposed surface of the RSV F protein, and they bound within the hydrophobic pocket through π–π stacking and cation-π interactions with F137, F140, and F488. Furthermore, compounds **94c** and **94d** showed a favorable profile in terms of lipophilicity, with a log *P* value below 5 (Lipinski rules) and also demonstrated complete absorption at the human intestinal membrane compared to the reference compound, exhibiting greater oral bioavailability and lower binding to plasma proteins. SAR analysis revealed that regarding *Influenza A* and *Corona virus*, the activity is attributed to thiosemicarbazone especially when compared with the benzyl ring; the nature of the substituent also does not have a significant effect on antiviral activity as the unsubstituted derivative (H) **94b** had high potency comparable with electron-withdrawing (Cl) **94a**. Furthermore, compounds featuring 2-benzotriazol in addition to thiosemicarbazone and hydrazone moieties **94c** and **94d** showed selective potency against *Respiratory syncytial virus* (RSV), comparable to the approved antiviral drug ribavirin.[102]

Novel substituted benzimidazole derivatives were designed by Bečet *et al.* and evaluated against different viruses as *Human corona virus*, *Influenza virus*, *Yellow fever virus*, *Zika virus* and *Sindbis virus* (Fig. 33). Moreover, they studied the impact of the synthesized compounds on the biological activity of substituents positioned at N atom of the benzimidazole nuclei and type of substituents attached to the phenyl ring. Compounds **95a**

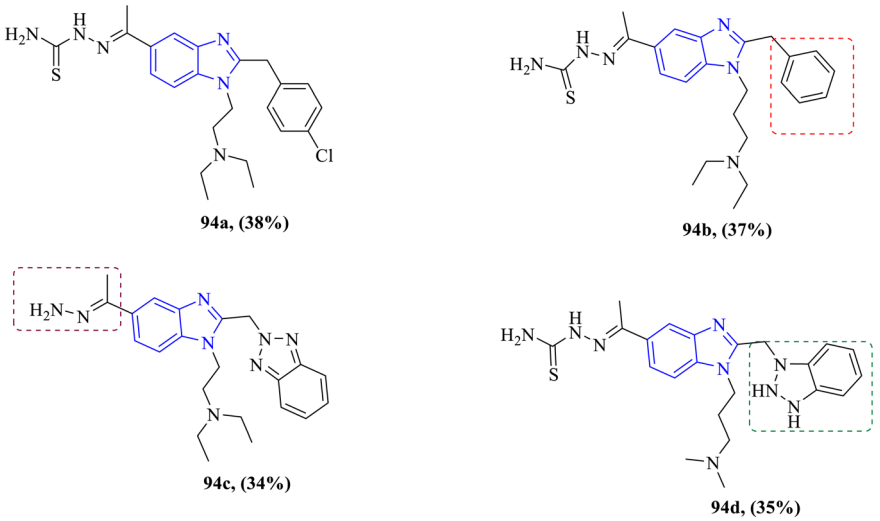

Fig. 32 Benzimidazole derivatives **94a–d** evaluated for antiviral activity against RSV, *Influenza*, and *Corona virus*.

Table 29 EC_{50} values of synthesized benzimidazole derivatives **94a–d** against RSV, *Influenza*, and *Corona virus*

	Effective concentration 50 (μM)		
Compound	*Influenza virus*	*Corona virus*	*Respiratory syncytial virus*
94a	38	56	—
94b	25	38	—
94c	—	—	7
94d	—	—	2.4
Ribavirin	7.5	7.5	6.7

and **95b** displayed high selectivity against *Zika virus* through inhibition of its replication through inhibition of RNA-dependent RNA polymerase with EC_{50} = 43.1 μM and 46.4 μM, respectively, if compared with the EC_{50} of the reference drug ribavirin >250 μM, while compounds **95c** and **95d** showed poor activity against all tested viral strains with EC_{50} > 100 μM (Table 30). The SAR studies revealed that novel benzimidazole derivatives bearing free NH_2 group at position 2 retain or increase antiviral activity. Also cyano group is optimal for activity at position 5 and shifting in positioning at 6-position badly affect potency while variation in substituents at position 1 with aliphatic chains afford derivatives **95a** with high potent antiviral activity than substitution with phenyl ring **95b**. While N-substitution with Schiff base derivatives such as bearing 4-*N*,*N*-dimethyl amino- or 4-*N*,*N* diethylamino-2-hydroxyohenyl ring **95c** and **95d** proved to be lacking any antiviral activity.[103]

In 2023, Srivastava *et al.* designed and synthesized novel pyrimidine hybrids and screened them for their antiviral activity against different viruses such as *Human immunodeficiency virus* (HIV), *Para-influenza-3 virus*, *Reovirus*, *Sindbis virus*, *Coxsackie virus* and *Yellow fever virus* (Fig. 34). Compound **96a** displayed high selectivity and potency against *Coxsackie virus* acting by inhibition of its replication through inhibition of

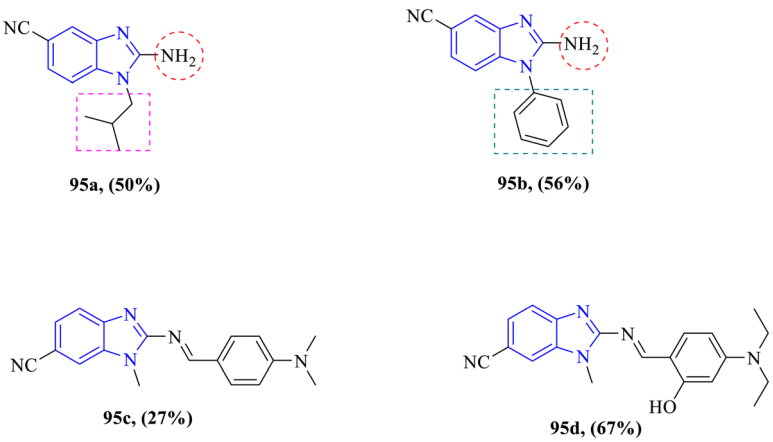

Fig. 33 Benzimidazole analogs **95a–d** developed for antiviral testing against *Zika virus*.

Table 30 Antiviral activity (EC_{50}) of benzimidazole derivatives **95a–d** against *Zika virus*

Compound	Effective concentration 50 (μM)
	Zika virus
95a	43.1
95b	46.4
95c	>100
95d	>100
Ribavirin	>250

Table 31 EC_{50} values of designated benzimidazole **96a–e** against *Coxsackie virus* and *HIV*

Compound	Effective concentration 50 ($\mu g\ mL^{-1}$ & μM^{-1})	
	Coxsackie virus	*HIV*
96a	0.026	—
96b	—	>100
96c	—	>100
96d	—	6.65
96e	—	15.82
Ribavirin	>250	>250

RNA-dependent RNA polymerase leading to mutagenesis and suppression of viral replication with outstanding $EC_{50} = 0.026$ μM comparable to the $EC_{50} > 250$ μM of the reference drug ribavirin. Furthermore, compounds **96d** and **96e** exhibited excellent activity against *HIV* with IC_{50} values of 6.65 $\mu g\ mL^{-1}$ and 15.82 $\mu g\ mL^{-1}$, respectively, which indicated them as promising anti-HIV agents. While compounds **96b** and **96c** showed poor antiviral activity against all tested viruses with $IC_{50} > 100\ \mu g\ mL^{-1}$ (Table 31). Notably, molecular modelling studies revealed that compounds **96d** and **96e** exhibited π–π interactions with Tyr318 at a distance of 5.0 A° and π–π and π–cation interactions with Tyr318 and Lys103 amino acid residues, respectively, in the hydrophobic pocket of RT protein. Moreover, Molecular Dynamics (MD) Simulation was simulated over 50 ns to support docking studies, revealing that compound **96d** have higher stability than HIV-RT:nevirapine. In addition, the physicochemical properties and ADMET prediction for the designated compound **96d** displayed good oral bioavailability with high profile safety margin. SAR analysis revealed that antiviral activity against *Coxsackie virus* based on the phenyl ring at position 2 must be free of any substitutions and pyrimidine at the N1 of the benzimidazole core **96a**. Additionally, for anti-HIV activity, the introduction of halogens such as chlorine atom at *para* position of phenyl ring substituted from benzimidazole scafold at position 2, along with the incorporation of a five-membered ring at position 2 were found to be favorable. Furthermore, methyl substitution at position 5 of the N-1 pyrimidine ring enhanced the activity, as observed in compounds **96d** and **96e**.[104]

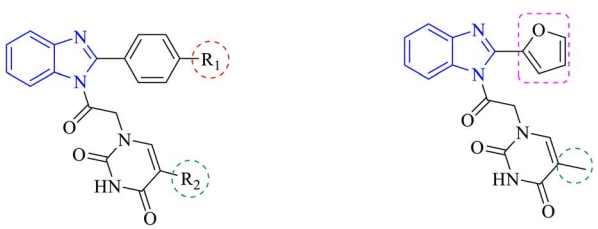

96a

96a: R1= H, R2= H, (52%)
96b: R1= H, R2= CH_3, (55%)
96c: R1= Cl, R2= H, (50%)
96d: R1= Cl, R2= CH_3, (57%)

96e, (58%)

Fig. 34 Benzimidazole hybrids **96a–e** evaluated for antiviral activity against *Coxsackie virus* and *HIV*.

3 General structure–activity relationship (SAR) study

The structure–activity relationship (SAR) describes the relation between a drug molecule's chemical or three-dimensional structure and its biological activity. This relationship is explored by altering the compound's structure to observe changes in its biological activity or potency. Specifically, the introduction of new functional groups and variations in their positions on the parent nucleus of a biologically active compound are evaluated to assess their impact on biological effects.

Antibacterial activity of benzimidazoles can be affected by:

• Metal complexation of benzimidazoles with metals such as nickel (Ni), particularly when substituted at position 2 as in compound **61a**, significantly enhances DNA intercalation and antibacterial activity.

• *Meta*-substituents on the 2-phenyl ring of benzimidazole like 3-$NHSO_2CH_3$ in compound **62a** enhance the antibacterial potency, whereas *para*-substituents in compound **62d** diminish activity.

• Unsubstituted amidino groups as in compound **63a** in 5-position contribute to broad-spectrum antibacterial activity. Moreover, the incorporation of lipophilic groups like isopropyl in compound **63c** increases selectivity towards Gram-positive bacteria, especially MRSA.

• Introduction of electron-withdrawing groups as Cl and CF_3 in position-5 in compounds **72a** and **72b** significantly boosts antibacterial potency, while electron-donating groups like methyl in compound **72c** reduce activity.

• Molecular hybridization with other heterocycles (*e.g.*, quinazoline and triazole in compound **70a**) at position-2 enhances the antibacterial activity.

• Aliphatic ester chains on the triazole ring at position-2 in compound **66a** had broad-spectrum activity, while bulkier or aromatic groups in compound **66b** tend to narrow the spectrum towards Gram-positive bacteria.

• The incorporation of hydrophilic groups such as carboxylic acid in compound **68a** improves activity compared to other lipophilic substitutions.

• Bulky groups such as methoxy group at position 1 on the heterocycle as in compound **73d** negatively impact antibacterial activity.

Antifungal activity of benzimidazoles can be affected by:

• Substitution at position 5 with bulky benzoyl groups in compounds **78a** and **78b** significantly enhances antifungal potency. In contrast, applying a simplification strategy on the structure as in compound **78c** reduces the activity.

• Introduction of hydrophilic groups on the 2-phenyl ring of benzimidazole core as hydroxyl groups in compound **84a** or free of substitution in **84c** derivative improve activity, while lipophilic groups such as bromine in **84b** diminish efficacy.

• Electron-withdrawing groups such as chlorine in compounds **79a–c** and fluorine in compounds **75a** and **75b** at position 2 of the phenyl ring were associated with enhanced antifungal activity. Conversely, substitution with electron-donating groups like methoxy or methyl, as in **74d** and **82a**, reduced antifungal potency.

• Introducing triazole and oxadiazole substituents at position 2 of the benzimidazole scaffold was found to be essential for antifungal activity, enhancing binding affinity to HEM and increasing efficacy against the tested fungal strains, as observed in compounds **76a**, **78a**, and **81a–c**.

• Molecular hybridization with thiazole and morpholine at position-2 in compounds **80a–c** improves activity, especially against *C. neoformans* as morpholine increases membrane penetration. Moreover, introduction of a hydrazone moiety at position-5 in **83a–c** derivatives enhances selectivity and potency, particularly with chlorine substitution at position 4 of the phenyl ring.

• Planar conformations (*e.g.* in compounds **77a** and **77b**) enhance π–π interactions with fungal enzymes, thus enhancing the antifungal activity.

Dual antibacterial and antifungal activities of benzimidazoles can be affected by:

• Short aliphatic chains (ethyl) at position-1 on the benzimidazole core enhance antibacterial activity as in compound **85a** and **91a** whereas longer chains reduce it in compound **85d**, **91b** and **91c**.

• Benzimidazole incorporated with benzoyl moieties affected by substitution properties as electron withdrawing groups as bromine and nitro on the phenyl ring in derivatives **88a–d** significantly enhance antimicrobial activity, while electron donating groups like methyl and methoxy in compounds **88e–f** reduce it.

• In carvacrol-based benzimidazole, bioisosteric replacement of the phenyl ring with a pyridine ring in the **89c** derivative enhances the activity against *S. aureus*, while the introduction of an electron-donating group like methyl group in compound **89b** positively affected the activity against *E. coli*, furthermore introduction of halogens at position 6 enhance the activity against *C. albicans* as in compounds **89e–f**.

• The design of benzimidazole–chalcone hybrids at position 2 generally resulted in enhanced antimicrobial activity if incorporated with electron donating groups as CH_3 group **90a** on the other hand electron withdrawing groups like F, Cl diminished activity **90b** and **90c** or with pyrimidine moieties incorporated with electron with drawing group Cl improve antibacterial activity **92b** while introduction electron donating group CH_3 enhance antifungal activity **92c**.

Antiviral activity of benzimidazoles can be affected by:

• Molecular hybridization with a thiosemicarbazone moiety at position-5 and the presence of an unsubstituted phenyl ring at position-2 are essential for antiviral activities against *Influenza A* and *Corona virus* **94b** than **94a**.

• The introduction of a benzotriazole moiety at position-2 enhances the selectivity for RSV (compounds **94c** and **94d**).

• For anti-Zika virus activity, a free $-NH_2$ group at position 2 is essential for optimal efficacy as compounds **95a** and **95b** than other substituted compounds **95c** and **95d**, also presence of cyano group at position-5 is optimal for antiviral activity, moreover, N1 substitution with aliphatic chains **95a** has favored antiviral activity over phenyl rings **95b**.

• Introducing a pyrimidine moiety at position 1 of the benzimidazole ring, along with an unsubstituted phenyl ring at position 2, as in compound **96a**, was found to be crucial for activity against *Coxsackie virus*. In the case of HIV, substitution at the *para*-position of the phenyl ring with a large radius atom such as chlorine, as in compound **96d**, enhanced antiviral activity.

4 Conclusion and future prospects

The period from 2018 to 2024 has witnessed substantial advancements in the synthesis and antimicrobial evaluation of benzimidazole derivatives, reaffirming their significance in medicinal chemistry. Novel synthetic methodologies, particularly those aligned with green chemistry principles, have facilitated efficient and sustainable production of these compounds. Structural modifications and the development of hybrid molecules have demonstrated remarkable antimicrobial activity, even against multidrug-resistant pathogens. SAR studies have further refined our understanding of structure–activity relationships, paving the way for the rational design of highly potent derivatives. Despite these achievements, challenges remain, such as the need for improved selectivity, reduced toxicity, and enhanced pharmacokinetic profiles for clinical applications. Future research should focus on the exploration of benzimidazole-based nanomaterials and drug delivery systems hold promise for enhancing the therapeutic efficacy and overcoming resistance mechanisms. The continued emphasis on interdisciplinary approaches and collaborative efforts will be crucial in unlocking the full potential of benzimidazoles as next-generation antimicrobial agents, addressing the global crisis of antimicrobial resistance.

Data availability

No primary research results, software or code have been included and no new data were generated or analyzed as part of this review.

Conflicts of interest

There are no conflicts to declare.

References

1 Z. Hosseinzadeh, A. Ramazani and N. Razzaghi-Asl, Anti-cancer nitrogen-containing heterocyclic compounds, *Curr. Org. Chem.*, 2018, **22**(23), 2256–2279.
2 T. Qadir, *et al.*, A review on medicinally important heterocyclic compounds, *Open Med. Chem. J.*, 2022, **16**(1), e187410452202280.
3 M. Hossain and A. K. Nanda, A review on heterocyclic: Synthesis and their application in medicinal chemistry of imidazole moiety, *Science*, 2018, **6**(5), 83–94.
4 V. J. Ram, *et al.*, *The Chemistry of Heterocycles: Nomenclature and Chemistry of Three to Five Membered Heterocycles*, Elsevier, 2019.
5 K. Singh, *et al.*, Insights into the structure activity relationship of nitrogen-containing heterocyclics for the development of antidepressant compounds: An updated review, *J. Mol. Struct.*, 2021, **1237**, 130369.
6 C. Verma, *et al.*, Coordination bonding and corrosion inhibition potential of nitrogen-rich heterocycles: Azoles and triazines as specific examples, *Coord. Chem. Rev.*, 2023, **488**, 215177.
7 S. Banerjee, *et al.*, A critical review of benzimidazole: Sky-high objectives towards the lead molecule to predict the future in medicinal chemistry, *Results Chem.*, 2023, **6**, 101013.
8 Y. N. A. Soh, *et al.*, Composition and biotransformational changes in soluble microbial products (SMPs) along an anaerobic baffled reactor (ABR), *Chemosphere*, 2020, **254**, 126775.
9 H. Hernández-López, C. J. Tejada-Rodríguez and S. Leyva-Ramos, A panoramic review of benzimidazole derivatives and their potential biological activity, *Mini-Rev. Med. Chem.*, 2022, **22**(9), 1268–1280.
10 S. K. Manna, T. Das and S. Samanta, Polycyclic benzimidazole: Synthesis and photophysical properties, *ChemistrySelect*, 2019, **4**(30), 8781–8790.
11 P. K. Singh and O. Silakari, Benzimidazole: journey from single targeting to multitargeting molecule, in *Key Heterocycle Cores for Designing Multitargeting Molecules*, Elsevier, 2018, pp. 31–52.
12 X. Yang, *et al.*, A New Discovery towards Novel Skeleton of Benzimidazole-Conjugated Pyrimidinones as Unique Effective Antibacterial Agents, *Chin. J. Chem.*, 2022, **40**(22), 2642–2654.
13 H. A. AlDifar, *et al.*, Synthesis of Benzimidazole and Phthaloylamino Acid derivatives and Antibacterial Activity, *J. Med. Chem. Sci.*, 2023, **6**, 1975–1984.
14 V. Kamat, *et al.*, Synthesis, molecular docking, antibacterial, and anti-inflammatory activities of benzimidazole-containing tricyclic systems, *J. Chin. Chem. Soc.*, 2021, **68**(6), 1055–1066.
15 K. Mahmood, *et al.*, Synthesis, characterization and biological evaluation of novel benzimidazole derivatives, *J. Biomol. Struct. Dyn.*, 2020, **38**(6), 1670–1682.
16 E. Mulugeta and Y. Samuel, Synthesis of Benzimidazole-Sulfonyl Derivatives and Their Biological Activities, *Biochem. Res. Int.*, 2022, **2022**(1), 7255299.
17 B. T. B. Hue, *et al.*, Benzimidazole derivatives as novel zika virus inhibitors, *ChemMedChem*, 2020, **15**(15), 1453–1463.
18 X. Huo, *et al.*, Design, synthesis, *in vitro* and *in vivo* anti-respiratory syncytial virus (RSV) activity of novel oxizine fused benzimidazole derivatives, *Eur. J. Med. Chem.*, 2021, **224**, 113684.
19 J. C. Sánchez-Salgado, *et al.*, Systematic search for benzimidazole compounds and derivatives with antileishmanial effects, *Mol. Diversity*, 2018, **22**, 779–790.
20 N. Razzaghi-Asl, *et al.*, Insights into the current status of privileged N-heterocycles as antileishmanial agents, *Mol. Diversity*, 2020, **24**, 525–569.
21 G. A. Dziwornu, *et al.*, Antimalarial benzimidazole derivatives incorporating phenolic mannich base side chains inhibit microtubule and hemozoin formation: structure–activity relationship and *in vivo* oral efficacy studies, *J. Med. Chem.*, 2021, **64**(8), 5198–5215.
22 M. Leshabane, *et al.*, Benzimidazole derivatives are potent against multiple life cycle stages of Plasmodium falciparum malaria parasites, *ACS Infect. Dis.*, 2021, **7**(7), 1945–1955.
23 V. M. Patel, *et al.*, N-Mannich bases of benzimidazole as a potent antitubercular and antiprotozoal agents: Their synthesis and computational studies, *Synth. Commun.*, 2020, **50**(6), 858–878.
24 A. Moreno-Herrera, *et al.*, Recent advances in the development of broad-spectrum antiprotozoal agents, *Curr. Med. Chem.*, 2021, **28**(3), 583–606.
25 J.-Y. Chai, B.-K. Jung and S.-J. Hong, Albendazole and mebendazole as anti-parasitic and anti-cancer agents: an update, *Korean J. Parasitol.*, 2021, **59**(3), 189.
26 N. T. Chung, V. C. Dung and D. X. Duc, Recent achievements in the synthesis of benzimidazole derivatives, *RSC Adv.*, 2023, **13**(46), 32734–32771.
27 S. Bai, *et al.*, Research Progress on Benzimidazole Fungicides: A Review, *Molecules*, 2024, **29**(6), 1218.
28 J. Jacob, *et al.*, Clinical efficacy and safety of albendazole and other benzimidazole anthelmintics for rat lungworm disease (neuroangiostrongyliasis): a systematic analysis of clinical reports and animal studies, *Clin. Infect. Dis.*, 2022, **74**(7), 1293–1302.
29 M. Budetić, *et al.*, Review of Characteristics and Analytical Methods for Determination of Thiabendazole, *Molecules*, 2023, **28**(9), 3926.
30 I. Celik, *et al.*, Synthesis, Molecular Docking, Dynamics, Quantum-Chemical Computation, and Antimicrobial Activity Studies of Some New Benzimidazole–Thiadiazole Hybrids, *ACS Omega*, 2022, **7**(50), 47015–47030.
31 S. B. F. Fawzi, *et al.*, Benzimidazole and Its Derivatives: Exploring Their Crucial Role in Medicine and Agriculture: A Short Review, *Al-Kitab J. for Pure Sci.*, 2024, **8**(02), 125–137.
32 B. Pathare and T. Bansode, biological active benzimidazole derivatives, *Results Chem.*, 2021, **3**, 100200.

33 R. S. Keri, *et al.*, Comprehensive review in current developments of benzimidazole-based medicinal chemistry, *Chem. Biol. Drug Des.*, 2015, **86**(1), 19–65.
34 M. Faheem, *et al.*, A review on the modern synthetic approach of benzimidazole candidate, *ChemistrySelect*, 2020, **5**(13), 3981–3994.
35 Y. Bansal and O. Silakari, The therapeutic journey of benzimidazoles: A review, *Bioorg. Med. Chem.*, 2012, **20**(21), 6208–6236.
36 N. D. Mahurkar, *et al.*, Benzimidazole: A Versatile Scaffold for Drug Discovery and Beyond-A Comprehensive Review of Synthetic Approaches and Recent Advancements in Medicinal Chemistry, *Results Chem.*, 2023, 101139.
37 M. S. Vasava, *et al.*, Benzimidazole: A milestone in the field of medicinal chemistry, *Mini-Rev. Med. Chem.*, 2020, **20**(7), 532–565.
38 V. A. S. Pardeshi, *et al.*, A review on synthetic approaches of benzimidazoles, *Synth. Commun.*, 2021, **51**(4), 485–513.
39 S. Thapa, S. L. Nargund and M. S. Biradar, A systematic review on diverse synthetic route and pharmacological activities of benzimidazole as optimized lead, *J. Ultra Chem.*, 2022, **18**(2), 24–36.
40 M. Patel, *et al.*, A Review of Approaches to the Metallic and Non-Metallic Synthesis of Benzimidazole (BnZ) and Their Derivatives for Biological Efficacy, *Molecules*, 2023, **28**(14), 5490.
41 S. I. Alaqeel, Synthetic approaches to benzimidazoles from o-phenylenediamine: A literature review, *J. Saudi Chem. Soc.*, 2017, **21**(2), 229–237.
42 M. R. Poor Heravi and M. Ashori, Boric acid catalyzed convenient synthesis of benzimidazoles in aqueous media, *J. Chem.*, 2013, **2013**(1), 496413.
43 A. Mehra and R. Sangwan, Synthesis and Pharmacological Properties of the Benzimidazole Scaffold: A Patent Review, *ChemistrySelect*, 2023, **8**(45), e202300537.
44 P. P. Nair, A. Jayaraj and C. A. Swamy P, Recent advances in benzimidazole based NHC-metal complex catalysed cross-coupling reactions, *ChemistrySelect*, 2022, **7**(4), e202103517.
45 B. Zou, Q. Yuan and D. Ma, Synthesis of 1, 2-disubstituted benzimidazoles by a Cu-catalyzed cascade aryl amination/condensation process, *Angew. Chem., Int. Ed.*, 2007, **46**(15), 2598–2601.
46 K. Das, A. Mondal and D. Srimani, Selective synthesis of 2-substituted and 1, 2-disubstituted benzimidazoles directly from aromatic diamines and alcohols catalyzed by molecularly defined nonphosphine manganese (I) complex, *J. Org. Chem.*, 2018, **83**(16), 9553–9560.
47 T. B. Nguyen, L. P. A. Nguyen and T. T. T. Nguyen, Sulfur-Catalyzed Oxidative Coupling of Dibenzyl Disulfides with Amines: Access to Thioamides and Aza Heterocycles, *Adv. Synth. Catal.*, 2019, **361**(8), 1787–1791.
48 L. A. Nguyen, P. Retailleau and T. B. Nguyen, Elemental Sulfur/DMSO-Promoted Multicomponent One-pot Synthesis of Malonic Acid Derivatives from Maleic Anhydride and Amines, *Adv. Synth. Catal.*, 2019, **361**(12), 2864–2869.
49 J. Mokhtari and A. H. Bozcheloei, One-pot synthesis of benzoazoles *via* dehydrogenative coupling of aromatic 1, 2-diamines/2-aminothiophenol and alcohols using Pd/Cu-MOF as a recyclable heterogeneous catalyst, *Inorg. Chim. Acta*, 2018, **482**, 726–731.
50 V. Sankar, *et al.*, Metal–organic framework mediated expeditious synthesis of benzimidazole and benzothiazole derivatives through an oxidative cyclization pathway, *New J. Chem.*, 2020, **44**(3), 1021–1027.
51 D. M. Dissanayake and A. K. Vannucci, Transition-Metal-Free and Base-Free Electrosynthesis of 1 H-Substituted Benzimidazoles, *ACS Sustain. Chem. Eng.*, 2018, **6**(1), 690–695.
52 K. Kant, *et al.*, Recent Advancements in Strategies for the Synthesis of Imidazoles, Thiazoles, Oxazoles, and Benzimidazoles, *ChemistrySelect*, 2023, **8**(47), e202303988.
53 X. Liu, *et al.*, CN bond formation and cyclization: A straightforward and metal-free synthesis of N-1-alkyl-2-unsubstituted benzimidazoles, *Tetrahedron Lett.*, 2019, **60**(15), 1057–1059.
54 H. Mostafavi, *et al.*, Synthesis of 1 H-1, 3-benzimidazoles, benzothiazoles and 3 H-imidazo [4, 5-c] pyridine using DMF in the presence of HMDS as a reagent under the transition-metal-free condition, *Chem. Pap.*, 2018, **72**, 2973–2978.
55 F. Feizpour, M. Jafarpour and A. Rezaeifard, A tandem aerobic photocatalytic synthesis of benzimidazoles by cobalt ascorbic acid complex coated on TiO_2 nanoparticles under visible light, *Catal. Lett.*, 2018, **148**, 30–40.
56 Z. Gan, *et al.*, Imidazolium chloride-catalyzed synthesis of benzimidazoles and 2-substituted benzimidazoles from o-phenylenediamines and DMF derivatives, *Tetrahedron*, 2018, **74**(52), 7450–7456.
57 S. K. Bagaria, N. Jangir and D. K. Jangid, Green and eco-compatible iron nanocatalysed synthesis of benzimidazole: A review, *Sustainable Chem. Pharm.*, 2023, **31**, 100932.
58 S. Singhal, *et al.*, Recent Trends in the Synthesis of Benzimidazoles From o-Phenylenediamine *via* Nanoparticles and Green Strategies Using Transition Metal Catalysts, *J. Heterocycl. Chem.*, 2019, **56**(10), 2702–2729.
59 N. Kaur, *et al.*, Metallovesicles as smart nanoreactors for green catalytic synthesis of benzimidazole derivatives in water, *J. Mater. Chem. A*, 2019, **7**(29), 17306–17314.
60 M. Nardi, *et al.*, A review on the green synthesis of benzimidazole derivatives and their pharmacological activities, *Catalysts*, 2023, **13**(2), 392.
61 A. Arya, V. Mishra and T. S. Chundawat, Green synthesis of silver nanoparticles from green algae (Botryococcus braunii) and its catalytic behavior for the synthesis of benzimidazoles, *Chem. Data Collect.*, 2019, **20**, 100190.
62 M. L. Di Gioia, *et al.*, Green synthesis of privileged benzimidazole scaffolds using active deep eutectic solvent, *Molecules*, 2019, **24**(16), 2885.

63 F. Shukla, M. Das and S. Thakore, Copper nanoparticles loaded polymer vesicles as environmentally amicable nanoreactors: a sustainable approach for cascading synthesis of benzimidazole, *J. Mol. Liq.*, 2021, **336**, 116217.
64 L. Ravindar, *et al.*, Cross-Coupling of C−H and N−H Bonds: A Hydrogen Evolution Strategy for the Construction of C−N Bonds, *Eur. J. Org Chem.*, 2022, **2022**(31), e202200596.
65 D. Kaldhi, *et al.*, Organocatalytic oxidative synthesis of C2-functionalized benzoxazoles, naphthoxazoles, benzothiazoles and benzimidazoles, *Tetrahedron Lett.*, 2019, **60**(3), 223–229.
66 T. T. Bui and H. K. Kim, Recent Advances in Photo-mediated Radiofluorination, *Chem.–Asian J.*, 2021, **16**(16), 2155–2167.
67 T. Montini, *et al.*, Sustainable photocatalytic synthesis of benzimidazoles, *Inorg. Chim. Acta*, 2021, **520**, 120289.
68 G. Kumaraswamy, *et al.*, An efficient photocatalytic synthesis of benzimidazole over cobalt-loaded TiO2 catalysts under solar light irradiation, *J. Photochem. Photobiol., A*, 2022, **429**, 113888.
69 H. N. Abdelhamid, I. M. Mekhemer and A.-A. M. Gaber, Metal-organic frameworks (MOFs)-derived ZrOSO4@ C for photocatalytic synthesis of benzimidazole derivatives, *Mol. Catal.*, 2023, **548**, 113418.
70 M. Gaba and C. Mohan, Development of drugs based on imidazole and benzimidazole bioactive heterocycles: recent advances and future directions, *Med. Chem. Res.*, 2016, **25**, 173–210.
71 R. M. LoPachin and T. Gavin, Molecular mechanisms of aldehyde toxicity: a chemical perspective, *Chem. Res. Toxicol.*, 2014, **27**(7), 1081–1091.
72 D. Hernández-Romero, *et al.*, First-row transition metal compounds containing benzimidazole ligands: An overview of their anticancer and antitumor activity, *Coord. Chem. Rev.*, 2021, **439**, 213930.
73 K. Mahmood, *et al.*, Synthesis, DNA binding and antibacterial activity of metal (II) complexes of a benzimidazole Schiff base, *Polyhedron*, 2019, **157**, 326–334.
74 M. A. Argirova, *et al.*, New 1 H-benzimidazole-2-yl hydrazones with combined antiparasitic and antioxidant activity, *RSC Adv.*, 2021, **11**(63), 39848–39868.
75 E. M. Dokla, *et al.*, Development of benzimidazole-based derivatives as antimicrobial agents and their synergistic effect with colistin against gram-negative bacteria, *Eur. J. Med. Chem.*, 2020, **186**, 111850.
76 A. Bistrović, *et al.*, Synthesis, anti-bacterial and anti-protozoal activities of amidinobenzimidazole derivatives and their interactions with DNA and RNA, *J. Enzyme Inhib. Med. Chem.*, 2018, **33**(1), 1323–1334.
77 H. R. Rashdan, *et al.*, Synthesis, identification, computer-aided docking studies, and ADMET prediction of novel benzimidazo-1, 2, 3-triazole based molecules as potential antimicrobial agents, *Molecules*, 2021, **26**(23), 7119.
78 L. Deswal, *et al.*, Synthesis, antimicrobial and α-glucosidase inhibition of new benzimidazole-1, 2, 3-triazole-indoline derivatives: a combined experimental and computational venture, *Chem. Pap.*, 2022, **76**(12), 7607–7622.
79 A. Saber, *et al.*, New 1, 2, 3-triazole containing benzimidazolone derivatives: Syntheses, crystal structures, spectroscopic characterizations, Hirshfeld surface analyses, DFT calculations, anti-corrosion property anticipation, and antibacterial activities, *J. Mol. Struct.*, 2021, **1242**, 130719.
80 F. F. Al-Blewi, *et al.*, Design, synthesis, ADME prediction and pharmacological evaluation of novel benzimidazole-1, 2, 3-triazole-sulfonamide hybrids as antimicrobial and antiproliferative agents, *Chem. Cent. J.*, 2018, **12**, 1–14.
81 Y. Aparna, *et al.*, Synthesis and Antimicrobial Activity of Novel Bis-1, 2, 3-triazol-1 H-4-yl-substituted Aryl Benzimidazole-2-thiol Derivatives, *Russ. J. Gen. Chem.*, 2020, **90**, 1501–1506.
82 G. K. Kantar, *et al.*, Synthesis and antimicrobial activity of some new triazole bridged benzimidazole substituted phthalonitrile and phthalocyanines, *Rev. Roum. Chim.*, 2018, **63**(1), 59–65.
83 N. K. Nandwana, *et al.*, Design and synthesis of imidazo/benzimidazo [1, 2-c] quinazoline derivatives and evaluation of their antimicrobial activity, *ACS Omega*, 2018, **3**(11), 16338–16346.
84 M. Al-Majidi, *et al.*, Synthesis and Identification of Some New Derivatives of ([Benzyl Thio) Benzimidazole-N-(Methylene-5-Yl)]-4, 5-Di Substituted 1, 2, 4-Triazole and Evaluation of Their Activity as Antimicrobial and Anti-Inflammatory Agents, *Iraqi J. Sci.*, 2021, **62**(4), 1054–1065.
85 K. El Gadali, *et al.*, Synthesis, structural characterization and antibacterial activity evaluation of novel quinolone-1, 2, 3-triazole-benzimidazole hybrids, *J. Mol. Struct.*, 2023, **1282**, 135179.
86 S. B. Korrapati, *et al.*, In-silico driven design and development of spirobenzimidazo-quinazolines as potential DNA gyrase inhibitors, *Biomed. Pharmacother.*, 2021, **134**, 111132.
87 D. Ashok, *et al.*, Conventional and microwave-assisted synthesis of new indole-tethered benzimidazole-based 1, 2, 3-triazoles and evaluation of their antimycobacterial, antioxidant and antimicrobial activities, *Mol. Diversity*, 2018, **22**, 769–778.
88 V. Mallikanti, *et al.*, Synthesis, antimicrobial activity and molecular docking of novel benzimidazole conjugated 1, 2, 3-triazole analogues, *Chem. Data Collect.*, 2023, **45**, 101034.
89 R. S. Kankate, P. S. Gide and D. P. Belsare, Design, synthesis and antifungal evaluation of novel benzimidazole tertiary amine type of fluconazole analogues, *Arabian J. Chem.*, 2019, **12**(8), 2224–2235.
90 A. E. Evren, İ. Çelik and U. A. Çevik, Synthesis, molecular docking, *in silico* ADME and antimicrobial activity studies of some new benzimidazole-triazole derivatives, *Cumhur. Sci. J.*, 2021, **42**(4), 795–805.
91 E. Ghobadi, *et al.*, Design, synthesis and biological activity of hybrid antifungals derived from fluconazole and mebendazole, *Eur. J. Med. Chem.*, 2023, **249**, 115146.

92 E. Güzel, *et al.*, Synthesis of benzimidazole-1, 2, 4-triazole derivatives as potential antifungal agents targeting 14α-demethylase, *ACS Omega*, 2023, **8**(4), 4369–4384.
93 S. Aaghaz, *et al.*, Synthesis, biological evaluation and mechanistic studies of 4-(1, 3-thiazol-2-yl) morpholine-benzimidazole hybrids as a new structural class of antimicrobials, *Bioorg. Chem.*, 2023, **136**, 106538.
94 U. A. Çevik, *et al.*, Synthesis, molecular modeling, quantum mechanical calculations and ADME estimation studies of benzimidazole-oxadiazole derivatives as potent antifungal agents, *J. Mol. Struct.*, 2022, **1252**, 132095.
95 E. C. Pham, *et al.*, N, 2, 6-Trisubstituted 1 H-benzimidazole derivatives as a new scaffold of antimicrobial and anticancer agents: design, synthesis, *in vitro* evaluation, and *in silico* studies, *RSC Adv.*, 2023, **13**(1), 399–420.
96 M. M. Morcoss, *et al.*, Design, synthesis, mechanistic studies and *in silico* ADME predictions of benzimidazole derivatives as novel antifungal agents, *Bioorg. Chem.*, 2020, **101**, 103956.
97 H. Chaurasia, *et al.*, Molecular modelling, synthesis and antimicrobial evaluation of benzimidazole nucleoside mimetics, *Bioorg. Chem.*, 2021, **115**, 105227.
98 Y. N. Wang, *et al.*, Discovery of Benzimidazole–Quinolone Hybrids as New Cleaving Agents toward Drug-Resistant Pseudomonas aeruginosa DNA, *ChemMedChem*, 2018, **13**(10), 1004–1017.
99 S. Yadav, *et al.*, Synthesis and evaluation of antimicrobial, antitubercular and anticancer activities of 2-(1-benzoyl-1 H-benzo [d] imidazol-2-ylthio)-N-substituted acetamides, *Chem. Cent. J.*, 2018, **12**, 1–14.
100 R. T. Bhoi, J. D. Rajput and R. S. Bendre, An efficient synthesis of rearranged new biologically active benzimidazoles derived from 2-formyl carvacrol, *Res. Chem. Intermed.*, 2022, 1–22.
101 H.-B. Liu, *et al.*, Novel aminopyrimidinyl benzimidazoles as potentially antimicrobial agents: Design, synthesis and biological evaluation, *Eur. J. Med. Chem.*, 2018, **143**, 66–84.
102 V. Francesconi, *et al.*, Synthesis and biological evaluation of novel (thio) semicarbazone-based benzimidazoles as antiviral agents against human respiratory viruses, *Molecules*, 2020, **25**(7), 1487.
103 A. Beč, *et al.*, Novel biologically active N-substituted benzimidazole derived Schiff bases: Design, synthesis, and biological evaluation, *Molecules*, 2023, **28**(9), 3720.
104 R. Srivastava, *et al.*, Exploring antiviral potency of N-1 substituted pyrimidines against HIV-1 and other DNA/RNA viruses: Design, synthesis, characterization, ADMET analysis, docking, molecular dynamics and biological activity, *Comput. Biol. Chem.*, 2023, **106**, 107910.